JPRS L/9164

27 June 1980

USSR Report

ELECTRONICS AND ELECTRICAL ENGINEERING

(FOUO 11/80)

FBIS FOREIGN BROADCAST INFORMATION SERVICE

NOTE

JPRS publications contain information primarily from foreign newspapers, periodicals and books, but also from news agency transmissions and broadcasts. Materials from foreign-language sources are translated; those from English-language sources are transcribed or reprinted, with the original phrasing and other characteristics retained.

Headlines, editorial reports, and material enclosed in brackets [] are supplied by JPRS. Processing indicators such as [Text] or [Excerpt] in the first line of each item, or following the last line of a brief, indicate how the original information was processed. Where no processing indicator is given, the information was summarized or extracted.

Unfamiliar names rendered phonetically or transliterated are enclosed in parentheses. Words or names preceded by a question mark and enclosed in parentheses were not clear in the original but have been supplied as appropriate in context. Other unattributed parenthetical notes within the body of an item originate with the source. Times within items are as given by source.

The contents of this publication in no way represent the policies, views or attitudes of the U.S. Government.

For further information on report content call (703) 351-2938 (economic); 3468 (political, sociological, military); 2726 (life sciences); 2725 (physical sciences).

APPROVED FOR RELEASE: 2007/02/08: CIA-RDP82-00850R000200090050-5

JPRS L/9164

27 June 1980

USSR REPORT

ELECTRONICS AND ELECTRICAL ENGINEERING

(FOUO 11/80)

CONTENTS

COMMUNICATIONS; COMMUNICATION EQUIPMENT INCLUDING RECEIVERS AND TRANSMITTERS; NETWORKS; RADIOPHYSICS; DATA TRANSMISSION AND PROCESSING; INFORMATION THEORY

An Antenna Servo System for a Laser Communications System 1

Basic Parameters of Bimetallic Waveguides for Radio-Relay Systems Operating in the 6 GHz Range 16

IKM-15 Rural Communications Equipment 24

RSL-DSh-ATS Interstation Communications Equipment for Rural Telephone Exchanges 39

OSCILLATORS, MODULATORS, GENERATORS

Analysis of the Effect of Ionizing Radiation on Self-Excited Oscillator Frequency Stability 46

PUBLICATIONS, INCLUDING COLLECTIONS OF ABSTRACTS

Papers on Electronic Technology 51

RADARS, RADIO NAVIGATION AIDS, DIRECTION FINDING, GYROS

Expanding the Limits of the Applicability of a Mathematical Radar Target Model 55

Multichannel Short-Range Noise Radar Stations with Integral Scan 59

UDC 621.369.946.2

AN ANTENNA SERVO SYSTEM FOR A LASER COMMUNICATIONS SYSTEM

Moscow RADIOTEKNIKA in Russian Vol 35, No 3, 1980 pp 25-34

[Article by I. M. Teplyakov]

[Text] The description and certain features of antenna guidance and tracking systems for an inter-satellite laser communication system are presented in [1, 2]. An analysis of a laser servo system with constant radiation of the laser beacon is made and optimization of a process for mutual search and guidance of antennas is examined in [3].

Let us examine a communication system with direct signal detection.

In many instances, the external background from the daytime sky, reflections from clouds, etc., are the main form of interference in laser communication systems, it being necessary to use a laser beacon in the short pulse radiation mode to suppress the background [4]. The angle tracking system may be of the single pulse or scanning type. A smaller pulse repetition frequency is required for the single pulse system [5], and, as a result of this, greater background suppression is possible; therefore it should be chosen for the laser system with direct signal detection.

The structural circuit for the single pulse angle tracking system of a laser beacon radiating a periodic sequence of short pulses is presented in a general form in Figure 1, where OA is the optical antenna; TsUUM is the elevation control circuit; TsUA is the azimuth control circuit; PR is the prismatic beam splitter; UI is the pulse amplifier; K is the key; OPI is the pulse sequence detector; SD is the range tracking unit and G_{s-i} is the gate pulse generator. A function diagram of an angle discriminator in one plane is shown in Figure 2, where UI is the pulse amplifier, while the shape of the discrimination curve is shown in

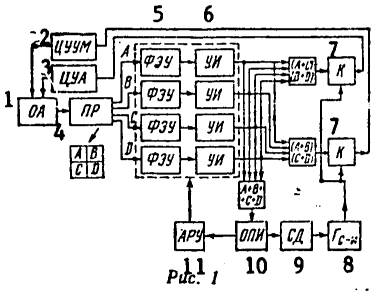

Рис. 1

Figure 1

Key to Figure 1:

1. OA-optical antenna
2. TsUUM-elevation control circuit
3. TsUA-azimuth control circuit
4. PR-prismatic beam-splitter
5. FEU-photoelectron multiplier
6. UI-pulse amplifier
7. K-key
8. G_{s-i}-gate pulse generator
9. SD-range tracking unit
10. OPI-pulse sequence detector
11. ARU-automatic amplification control

Figure 3 where $R_{s\ out}$ is the maximum signal strength at the output of the gating circuit; ϕ is the angular tracking error. We consider the discrimination curve to be linear over the section $\pm\delta$ where 2δ is the receiver's angle of vision.

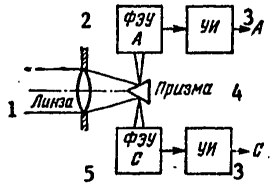

Рис. 2

Figure 2

Key to Figure 2:

1

1. Lens
2. FEU A-photoelectron multiplier A
3. UI-pulse amplifier
4. Prism
5. FEU C-photoelectron multiplier C

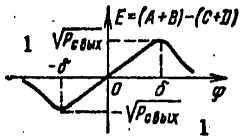

Рис. 3

Figure 3

Key to Figure 3:

$R_{s\ out}$-maximum signal strength at the output of the strobing circuit

Background Suppression. Let us examine the operation of an angle tracking system in one plane. Let us find the ratio of signal strength in the band of a tracking system ΔF_{sh} and compare this ratio $(R_s/R_{sh})_s$ with the corresponding expression for an angle tracking system with constant beacon signal. For a system with an uninterrupted signal, having a Poisson photoelectron current at the output of the photoelectron multiplier from the signal and the background [3,4]

$$\left(\frac{P_c}{P_m}\right)_c = \frac{(\eta\bar{n}_{c.n}T_{ш.n})^2}{\eta\bar{n}_{c.n}\bar{T}_{ш.n} + \eta\bar{n}_{ф}T_{ш.n}} = \frac{\eta E_c}{1+\bar{n}_{ф}/\bar{n}_{c.n}}, \qquad (1)$$

where $E_s = \bar{n}_{s.n}\ T_{sh.n} = \bar{n}_{s.n}/2\Delta F_{sh.n}$; $\Delta F_{sh.n} = 1/2T_{sh.n}$ is the noise band of the tracking system; η is the quantum yield of the photodectors; and $\bar{n}_{s.n}$ and $\bar{n}_f$ are the average number of signals and background photons incident on the prism per second, respectively. It is taken into consideration in [1] that the constant component from the background at the output of the photoelectron multiplier does not affect the operation of the tracking system; we assume that the power of noises at the outputs of circuits (A+C)-(B+D) and (A+B)-(C+D) is equal to the sum of the powers of the noises at their inputs.

Let us examine the pulse system. The spectral density of the noise (quantum and background) at the output of the gating circuit is equal to the [6]

$$N_0 = 2\varphi^2\tau^2/T = 2(\tau/T)^2\sigma^2T,$$

where τ is the pulse duration; T is the pulse repetition period;

$$\varphi^2 = k_p^2\eta(\bar{n}_c + \bar{n}_{ф})\tau$$

is the dispersion of pulse amplitude fluctuations; k_r is the amplification coefficient from the photocathode output to the output of the gating circuit; $\eta\bar{n}_s\tau$ and $\eta\bar{n}_f\tau$ are the average number of signal and background photoelectrons, respectively, for time τ at the photocathode output.

Then

$$N_0 = 2k_p^2(\tau/T)^2 T\eta\tau\left(\bar{n}_c + \bar{n}_\phi\right).$$

The maximum amplitude of the signal pulse at the output of the gating circuit is equal to $k_r \eta n_s \tau$ whereas the average strength of the useful signal is

$$\bar{P}_{s\cdot out} = \bar{P}_{out} = k_p^2(\tau/T)^2(\eta\bar{n}_c\tau)^2.$$

The ratio of the average signal strength to the strength of noise in the band ΔF_{sh} of a tracking system at the output of the gating circuit is equal to

$$\left(\frac{P_c}{P_m}\right)_c = \frac{k_p^2(\tau/T)^2(\eta\bar{n}_c\tau)^2}{N_0\Delta F_N} = \frac{(\tau/T)^2(\eta\bar{n}_c\tau)^2}{2(\tau/T)^2 T\eta\tau(\bar{n}_c+\bar{n}_\phi)\Delta F_m} = \frac{\eta\bar{n}_c\tau/T}{2\Delta F_m\left(1+\bar{n}_\phi/\bar{n}_c\right)}. \qquad (2)$$

We assume that the average signal strength at the input of the prism are identical for uninterrupted and pulse systems. Then, when $\Delta F_{sh\cdot n} = \Delta F_{sh}$, we obtain $E_s = \bar{n}_{s\cdot n} T_{sh\cdot n} = \bar{n}_s T_{sh}(\tau/T)$, where $\bar{n}_s = (\tau/T)\bar{n}_{s\cdot n}$. From (2) we have

$$\left(\frac{P_c}{P_m}\right)_c = \frac{\eta E_c}{1+(\bar{n}_\phi/\bar{n}_c)(\tau/T)} \qquad (3)$$

for a system with a pulse signal. It follows from Equations (1) and (3) that the power of the background in a pulse system is T/τ times less than for a system with a continuous signal, i.e. for an increase in background suppression it is necessary to reduce the duration of pulses τ and the frequency of pulse repetition $F_p = 1/T$.

Selection of pulse repetition frequency of the laser beacon.

Let the receiver be situated on a stabilized platform having an angular fluctuation $\theta(t)$ with a power spectrum $|\theta(iF)|^2 = \theta(F)$. We consider that restrictions on the pulse repetition frequency accumulate as angular fluctuations of this platform. We will describe the laser tracking system as a linear system with two integrators within the limits of the linear section of the angular discriminator aperature [3]. The structural circuit of the linear tracking system is shown in Figure 4 (where α and β are certain constants; the key element is ideal) and its equivalent transformation is shown in Figure 5, where

$$\theta^*(t) = \frac{1}{T}\theta(t) + \frac{2}{T}\sum_{l=1}^{\infty}\theta(t)\cos(2\pi l F_n t).$$

Let us examine the components of tracking system errors. In the first place, it distorts the spectrum $\theta(F)$ of the input signal $\theta(t)$; we will call this distortion the dynamic error analogy with the dynamic error of the continuous tracking system. In the second place, the constituents $\theta(t)\cos(2\pi l F_p t)$, with $l = 1, 2, \ldots$, which were formed as a result of a sampling of signal $\theta(t)$ will pass at the output of a pulse tracking system. These components at the output of the tracking system will create a sampling error which also determines the necessary values of F_p.

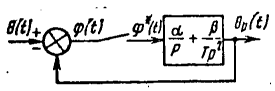

Puc. 4

Figure 4

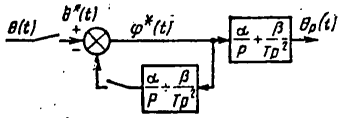

Puc. 5

Figure 5

Let us find the sampling error. Let the spectrum of the input signal strength be described by the expression $\theta(F) = 1/[1+F/F_s)^{2m}]$, where F_s is the width of the spectrum over the level of half power; m characterizes the decay rate of the spectrum with the frequency.

For an analysis of the sampling errors let us examine the structural circuit and Figure 6, where

$$G(p) = \alpha/p + \beta/Tp^2 = (\beta + \alpha Tp)/Tp^2; \quad G^*(z)$$

is the z-transform G(p); z = exp(pT); p = d/dt. On the other hand, we have $G^*(z) = z^{-1}G^*(z;1)$, where $G^*(z;1)$ is the modified z-transform of $G^*(z;\varepsilon)$ at $\varepsilon = 1$ for the function G(p). Using the z-transform tables, we find

$$G^*(z) = [(\alpha+\beta)z^{-1} - \alpha z^{-2}]/(1-z^{-1})^2.$$

Then the transfer function of the tracking system is equal to

$$X(p) = \frac{\theta_p(p)}{\theta^*(p)} = \frac{G(p)}{1+G^*(z)} = G(p)\frac{(1-z^{-1})^2}{1-(2-\alpha-\beta)z^{-1}+(1-\alpha)z^{-2}}.$$

The system's stability conditions determine the values of the coefficients [7] at $\alpha > 0$, $\beta > 0$, $2\alpha + \beta < 4$. For the transfer function with regard to error $Y^*(i\omega)$, we obtain

$$|Y^*(i\omega)|^2 = \frac{1}{|1+G^*(i\omega)|^2} = \frac{4(1-\cos\omega T)}{1+a_0^2+b_0^2-2(a_0+a_0b_0)\cos\omega T+2b_0\cos 2\omega T},$$

where $a_0 = 2 - \alpha - \beta$; $b_0 = 1 - \alpha$. At frequencies close to $\omega T = 2\pi l$, $l = 0, 1, 2, \ldots$, the denominator may be assumed to be equal to β^2. At $\alpha = \beta = 1$, we have the exact expression $|y^*(i\omega)|^2 = r(1 - \cos \omega T)$. The spectrum of the signal $\theta^*(t)$ and the amplitude frequency characteristic of the pulse $|y^*(iF)|$ and the continuous $|G(iF)|$ parts of the tracking system are presented in Figure 7.

Let us find the sampling error of a signal as the result of components $\theta(t) \cos(2\pi l F_p)$ at $l = 1, 2, \ldots$ passing through a quadripole with a transfer function X(p). The average square of the sampling error is

$$\sigma_l^2 = \int_0^\infty \left[\sum_{l=1}^{\infty} \frac{1}{T^2}\theta(F - lF_n)\right] |G(lF)|^2 |Y^*(lF)|^2 dF.$$

It may be seen from Figure 7 for an instance of small errors that the behavior of the functions $|G(iF)|^2$ and $|Y^*(iF)|^2$ in the area of frequencies $F \simeq iF_p$ at $l = 1, 2, \ldots$ is of interest. Then we have

$$|G(l\omega)|^2 = T^2 \frac{\beta^2 + \alpha^2(\omega T)^2}{(\omega T)^4}.$$

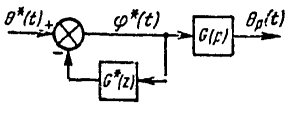

Рис. 6

Figure 6

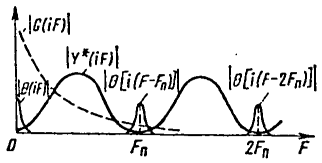

Рис. 7

Figure 7

At frequencies $F = lF_n$ at $l = 1, 2, \ldots$ $(\omega T)^2 >> 1$, one may consider that $|G(i\omega)|^2 \simeq \alpha^2/\omega^2$. Then $|G(ilF_p)|^2 = \alpha^2/(2\pi lF_p)^2$. For the function $|y^*(i\omega)|^2$ in the area of frequencies of $F = lF_p$ at $l = 1, 2, \ldots$ for small sampling errors

$$|Y^*(lF)|^2 = (4/\beta^2)(1 - \cos 2\pi FT)^2.$$

To sum up, we obtain

$$\sigma_l^2 = \frac{2\alpha^2}{\pi\beta^2}\int_0^\infty \theta(F)(1 - \cos 2\pi FT)^2\,dF \sum_{l=1}^{\infty} 1/l^2 =$$

$$= \frac{\alpha^2}{6\beta^2}\left[3\int_0^\infty \theta(F)\,dF - 4\int_0^\infty \theta(F)\cos(2\pi FT)\,dF + \int_0^\infty \theta(F)\cos(4\pi FT)\,dF\right].$$

The first integral [9] is $\int_0^\infty \theta(F)\,dF = \int_0^\infty \frac{dF}{1 + (F/F_c)^{2m}} = \frac{\pi F_c}{2m\sin(\pi/2m)}$.

The second and third integrals are calculated using the expression [8]

$$\int_0^\infty \frac{\cos(ay)\,dy}{b^{2m} + y^{2m}} = \frac{\pi}{2mb^{2m-1}} \sum_{k=1}^{m} \exp\left[-ab\sin\frac{(2k-1)\pi}{2m}\right] \times$$

$$\times \sin\left[\frac{(2k-1)\pi}{2m} + ab\cos\frac{(2k-1)\pi}{2m}\right],$$

Then, $\varepsilon_t^2 = \frac{8\sqrt{2}\pi^3\alpha^2}{9\beta^2}\left(\frac{F_c}{F_n}\right)^3$.

For $m > 2$ [9]

$$\sum_{k=1}^{m} \sin\frac{(2k-1)\pi}{2m} = \frac{1}{\sin(\pi/2m)};\ \sum_{k=1}^{m} \cos\frac{(2k-1)\pi}{m} = 0;$$

$$\sum_{k=1}^{m} \cos\frac{(2k-1)2\pi}{m} = 0;\ \sum_{k=1}^{m} \sin\frac{(2k-1)5\pi}{2m} = \frac{1}{\sin(5\pi/2m)}.$$

Then, $\varepsilon_t^2 = \frac{4\pi^4\alpha^2}{3\beta^2}\frac{\sin(\pi/2m)}{\sin(5\pi/2m)}\left(\frac{F_c}{F_n}\right)^4$.

Thus, for a minimal pulse repetition frequency at low values of ε_t we obtain

$$F_n \geqslant \begin{cases} (2\pi\alpha^2/3\beta^2\varepsilon_t^2)F_c & \text{при } m = 1; \\ 2\pi\left(\frac{\sqrt{2}\alpha^2}{9\beta^2\varepsilon_t^2}\right)^{1/3}F_c & \text{при } m = 2; \\ \frac{\pi}{\sqrt{\varepsilon_t}}\left[\frac{4\alpha^2}{3\beta^2}\frac{\sin(\pi/2m)}{\sin(5\pi/2m)}\right]^{1/4}F_c & \text{при } m > 2. \end{cases} \quad (4)$$

Tracking system parameters during transfer processes. After detection of the laser beacon signal, the angle tracking system is exposed to transient conditions before switching to the stationary tracking mode. It must be considered that a jump in angular velocity $d\theta(t)/dt$, equal to the sum of the angular speeds of the stabilized platform, and beacon displacement relative to the receiver affect the tracking system after detection of the signal. Further, we assume that the prediction for angular velocity $d\theta(t)/dt$ is not used to improve the angle tracking system characteristics.

High computational accuracy is not required in analyzing the transients; therefore, it is convenient to examine the angle tracking system as continuous. Let us analyze the structural circuit of the continuous tracking system with two integrators shown in Figure 8.

The tracking error is equal to $\varphi(p) = \theta(p)p^2/(p^2 + kp + k_1k)$.

Let us denote the angular translational velocity of the beacon relative to the receiver by $\Omega(t)$. For the jump in angular velocity $\Omega(t) = \Omega_0$ we have $\Omega(p) = \Omega_0/p$ and $\Omega(p) = \theta(P)/p = \Omega_0/p^2$. Then

$$\varphi(p) = \frac{\Omega_0}{p^2 + kp + k_1k} = \frac{\Omega_0}{\left(p + \frac{k}{2}\right)^2 + \frac{k^2}{4}\left(\frac{4k_1}{k} - 1\right)}.$$

where a = $2\pi T$; b = F_s; ab = $2\pi F_s/F_p$ for the second integral. Given small sampling errors, $2\pi F_s/F_p$ is $\ll 1$. Let us designate $(2k-1)\pi/2m = X$ ab = $\gamma \ll 1$. Then, restricting ourselves to members not greater than γ^4, we have

$$\exp\left[-ab\sin\frac{(2k-1)\pi}{2m}\right] = \exp(-\gamma\sin x) \approx 1 - \gamma\sin x + \\ + \frac{\gamma^2}{2}\sin^2 x - \frac{\gamma^3}{6}\sin^3 x + \frac{\gamma^4}{24}\sin^4 x;$$

$$\sin\left[\frac{(2k-1)\pi}{2m} + ab\cos\frac{(2k-1)\pi}{2m}\right] = \sin(x + \gamma\cos x) = \\ = \sin x\cos(\gamma\cos x) + \cos x\sin(\gamma\cos x).$$

Assuming

$$\sin(\gamma\cos x) \approx \gamma\cos x - \frac{\gamma^3}{6}\cos^3 x;$$

$$\cos(\gamma\cos x) \approx 1 - \frac{\gamma^2}{2}\cos^2 x + \frac{\gamma^4}{24}\cos^4 x,$$

we obtain

$$\exp(-\gamma\sin x)\sin(x + \gamma\cos x) \approx \sin x + \gamma\cos 2x + \\ + \frac{\gamma^2}{2}\sin x - \frac{\gamma^3}{6}\cos 4x + \frac{\gamma^4}{24}\sin 5x.$$

For m = 1, restricting ourselves to members not greater than γ,

$$\int_0^\infty \frac{\cos(ay)\,dy}{b^2 + y^2} \approx \frac{\pi}{2b}(1 - \gamma).$$

Let us introduce the normalized sampling error $\varepsilon_I^2 = \sigma_I^2 \Big/ \int_0^\infty \theta(F)\,dF.$

for m = 1 $\varepsilon_I^2 = \frac{2\pi a^2}{3\beta^2}\left(\frac{F_c}{F_n}\right).$

for m = 2, we have $\int_0^\infty \frac{\cos(ay)\,dy}{b^4 + y^4} \approx \frac{\pi}{4b^3}\left[2\left(1 + \frac{\gamma^2}{2}\right)\sin\frac{\pi}{4} + \frac{\gamma^3}{3}\right].$

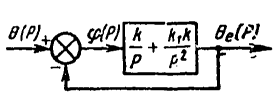

Figure 8

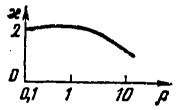

Figure 9

From the tables of inverse Laplace transforms we obtain

$$\varphi(t)=\begin{cases}\dfrac{\Omega_0}{k\sqrt{1-4k_1/k}}\left\{\exp\left[-\dfrac{k}{2}\left(1-\sqrt{1-4k_1/k}\right)t\right]-\right.\\ \left.-\exp\left[-\dfrac{k}{2}\left(1+\sqrt{1-4k_1/k}\right)t\right]\right\} & \text{for } 4k_1/k<1;\\ \Omega_0 t\exp\left(-\dfrac{k}{2}t\right) & \text{for } 4k_1/k=1;\\ \dfrac{2\Omega_0}{k\sqrt{4k_1/k-1}}\exp\left(-\dfrac{k}{2}t\right)\sin\left(\dfrac{k}{2}\sqrt{4k_1/k-1}\,t\right) & \text{for } 4k_1/k>1.\end{cases}$$

At a certain instant in time t_0 the error $\phi(t_0)$ is maximum. It is apparent that in order for there to be no break in tracking, the error should not exceed the aperture of the angle discriminator $\pm\delta$, i.e., $\phi(t_0)\leq\delta$. Let us designate $4k_1/k=\rho$.

From the condition $\phi(t_0)=\delta$ we will find the maximum permissable value of $\Omega_0=\Omega_z(\rho)$, still being tracked by the tracking system, i. e., we will determine the capture area for the system.

$$\Omega_3(\rho)\leqslant\begin{cases}\delta k\sqrt{1-\rho}\exp\left[\dfrac{\ln\left(\dfrac{1+\sqrt{1-\rho}}{1-\sqrt{1-\rho}}\right)}{2\sqrt{1-\rho}}\right]\Bigg/\left[\left(\dfrac{1+\sqrt{1-\rho}}{1-\sqrt{1-\rho}}\right)^{1/2}-\right.\\ \left.-\left(\dfrac{1+\sqrt{1-\rho}}{1-\sqrt{1-\rho}}\right)^{-1/2}\right] & \text{for } \rho<1;\\ \delta ek/2 & \text{for } \rho=1;\\ \dfrac{\delta k\sqrt{\rho}}{2}\exp\left(\dfrac{1}{\sqrt{\rho-1}}\operatorname{arc\,tg}\sqrt{\rho-1}\right) & \text{for } \rho>1.\end{cases}$$

The transfer function of the tracking system is equal to

$$K(p)=\theta_e(p)/\theta(p)=(kp+k_1k)/(p^2+kp+k_1k),$$

while the noise band is

$$\Delta F_{\text{ш}}=\frac{1}{2\pi}\int_0^\infty|K(i\omega)|^2d\omega=\frac{k}{4}\left(1+\frac{k_1}{k}\right)=\frac{k}{4}\left(1+\frac{\rho}{4}\right).$$

Let us examine the dimensionless value χ, characterizing the ratio of the capture area $\Omega_z(\rho)$ of the tracking system with regard to angular velocity to the system's noise band.

$$\chi=\frac{\Omega_3(\rho)}{2\delta\Delta F_{\text{ш}}}=\frac{\Omega_3(\rho)}{\Delta F_{\text{ш}}\Delta}=\frac{2\Omega_3(\rho)}{\delta k(1+\rho/4)},$$

where $\Delta = 2\delta$ is the receiver's angle of vision.

It follows from the graph of the change in χ (Figure 9) that within the braod area of values for ρ, one may consider that the band of the tracking system should be greater than or equal to

$$\Delta F_{sh} \geqslant \frac{\Omega_3(\rho)}{\pi\Delta} \approx \frac{\Omega_3(\rho)}{2\Delta} = \frac{\Omega_0}{2\Delta},$$

where $\Omega_z(\rho) \geq \Omega_0$; Ω_0 is the anticipated jump in angular velocity. In the general instance, the condition $\phi(t_0) < \delta$ should be satisfied with a reserve, i.e., $\phi(t_0) = \delta/r_0$, where $r_0 = 4 \div 6$ is the reserve coefficient. Then we finally obtain

$$\Delta F_{sh} \geqslant r_0 \frac{\Omega_0}{2\Delta}. \qquad (5)$$

The range tracking subsystem. This subsystem produces synchronizing pulses for gating the pulses being received from the angle tracking system signal. Let us consider that the structural circuit of a range tracking system is identical to the structural circuit for angle tracking and, given a high pulse repetition frequency, may be described by the circuit in Figure 8, whereas the aperture of the time discriminator is linear within the range $\pm\tau/2$, where τ is the duration of the pulses being received. Let us write an analogous expression for the noise band of the range tracking system as

$$\Delta F_{shR} \geqslant r_0 \frac{1}{2\tau}\left(\frac{\Delta F_D}{F_\rho}\right), \qquad (6)$$

where ΔF_D is the anticipated maximum difference in frequencies between the pulse repetition frequency of the slave pulse generator of the range tracking system at the initial instant of operation and the pulse repetition frequency of the signal being received. This difference in frequencies is caused by the discrepancy of the frequencies of the pulse generators at the transmitting and receiver ends of the laser line due to instability of the generators as well as by the Doppler shift in the pulse repetition frequency when the beacon is displaced with regard to the receiver.

The formula which was obtained arises from the following analogies. It is possible to express the aperture of the time discriminator in angular units $\Delta_\tau = 2\pi F_p \tau$, i.e., the aperture $2\pi F_p \tau$ of the range tracking system corresponds to the aperture Δ of the angle tracking system, while the angular velocity Ω_0 is the angular frequency $2\pi\Delta F_D$, from whence expression (6) follows:

The square of the relative root-mean-square of the angle tracking system's noise error is equal to [3] $(\sigma_{sh}/\delta)^2 = N_0 \Delta F_{sh}/P_{s.out}$.

Let us require that the necessary optical signal strength at the receiver input be identical for the angle tracking and range tracking channels. In this case, it is possible to write $\left(\frac{\sigma_{shR}}{\tau/2}\right)^2 = N_0 \Delta F_{shR}/P_{s.out}$.

for the square of the relative root-mean-square noise error with regard to range by analogy. It is logical to consider the relative root-mean-square noise errors of the angle and range tracking systems be identical. Hence, it follows that $\Delta F_{sh} = \Delta F_{shR}$. Using (5) and (6), we obtain the expression for the minimum pulse duration $\tau \geqslant \frac{\Delta}{\Omega_0}\frac{\Delta F_D}{F_n}$.

Dynamic and fluctuational errors of the angle tracking system. It is advisable to select the work mode of a tracking system close to the critical, whereby $(\alpha+\beta)^2 = 4\beta$ [7]. The squares of the amplitude-frequency characteristics of the system $|X(iF)|^2$ are presented in Figure 10 for several values of β (a mode close to the critical). They are adequately smooth for $\beta < 0.1$ and therefore the characteristics of the pulse system can be identical to the characteristics of a continuous system.

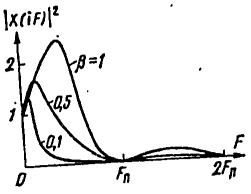

Puc. 10
Figure 10

It is possible to determine the dynamic error $\phi(t)$ from the structural diagram in Figure 6 given the input variable $\frac{1}{T}\theta(t)$. Let us examine the dynamic and noise errors of a tracking system in the range of values $\beta = 0.1 - 1$ where it is necessary to take the pulse nature of the system's operation into account. From Figure 6, the average square of the dynamic error is

$$\sigma_\varphi^2 = \int_0^\infty \frac{1}{T^2}\theta(F)|Y^*(iF)|^2 dF.$$

We consider that $F_s \ll \Delta F_{sh}$, which is fair, given small dynamic error. In this case, it is possible to assume that $|Y^*(iF)|^2 = (1/\beta^2)(1-\cos 2\pi FT)^2$.

Then

$$\sigma_\varphi^2 = \frac{4}{\beta^2 T^2}\int_0^\infty \theta(F)(1-\cos 2\pi FT)^2 dF.$$

On the other hand, it was earlier found that

$$\int_0^\infty \theta(F)(1-\cos 2\pi FT)^2 dF = \frac{3\beta^2}{a^2}\sigma_l^2.$$

Then the square of the dynamic error normed with regard to the strength of the input variable is equal to

$$\varepsilon_\varphi^2 = \sigma_\varphi^2/(1/T^2)\int_0^\infty \theta(F)dF = \frac{12}{a^2}\varepsilon_l^2. \qquad (7)$$

Let us determine the noise band of a pulse tracking system by the expression

$$\Delta F_{sh} = \frac{\frac{1}{2\pi}\int_0^\infty |Y^*(i\omega)|^2 |G(i\omega)|^2 d\omega}{|Y^*(0)G(0)|^2}$$

where $[y^*(0)G(0)]^2 = T^2$.

In particular, for $\alpha = \beta = 1$,

$$\Delta F_{sh} = \frac{1}{2\pi T^2}\int_0^\infty 4(1-\cos\omega T)^2 T^2 \frac{1+(\omega T)^2}{(\omega T)^4}\,d\omega = \frac{4}{3T} = \frac{4F_n}{3}.$$

It is possible to determine the noise band for other values of α and β by numerical integration. We assume that $F_p = \Psi\Delta F_{sh}$ where Ψ is a function of α and β. Then, using (4) and (7), assuming a peak factor of the process $\theta(t) = 4$ with a peak value of θ_m, we obtain $\varepsilon_\varphi = 4\sigma_\varphi/\theta_m$ and for $F_s \ll \Delta F_{sh}$ we get

$$\Delta F_{sh} = \begin{cases} (\pi/2\beta^2\psi)(\theta_m/\sigma_\varphi)^2 F_c & \text{for } m=1; \\ (\pi/\beta^{2/3}\psi)(2\sqrt{2}/3)^{1/3}(\theta_m/\sigma_\varphi)^{2/3}F_c & \text{for } m=2; \\ \frac{\pi}{\beta^{1/2}\psi}\left[\frac{\sin(\pi/2m)}{\sin(5\pi/2m)}\right]^{1/4}(\theta_m/\sigma_\varphi)^{1/2}F_c & \text{for } m>2. \end{cases} \tag{8}$$

Let us now examine the noise error determined by the general expression [3] $\sigma_N^2 = \delta^2/(P_s/P_{sh})_s$ for the tracking system. Using expression (2) we find

$$\left(\frac{\sigma_m}{\delta}\right)^2 = \frac{2\Delta F_m(1+\bar{n}_\phi/\bar{n}_c)}{\eta\bar{n}_c\tau/T} = \frac{\Delta F_m}{F_n}\frac{1+\bar{n}_\phi\tau/E_\tau}{\eta E_\tau},$$

where $E_\tau = \bar{n}_s\tau$ is the average number of photons of the signal at the input of the angle discriminator for time τ. From this equation the ratio of signal strength to noise strength at the output of the photocathode required for a single pulse is equal to

$$\frac{(\eta E_\tau)^2}{\eta E_\tau + \eta\bar{n}_F\tau} = 2\left(\frac{\delta}{\sigma_{sh}}\right)^2\frac{\Delta F_{sh}}{F_\rho} = \frac{2}{\psi}\left(\frac{\delta}{\sigma_{sh}}\right)^2. \tag{9}$$

We assume that $\bar{n}_s = P/hf$, where P is the optical signal strength at the input of the angle discriminator; h is Planck's constant; f is the optical signal frequency. The average optical signal strength at the input of the angle discriminator $P_{cp} = P\tau/T = hf\bar{n}_c\tau/T = F_n hf E_\tau$.
Using (8), we obtain

$$\eta E_\tau = c\left|1+(1+2\eta\bar{n}_F\tau/c)^{1/2}\right|,$$

where $c = (1/\psi)(\delta/\sigma_{sh})^2$. Then

$$P_{ave} = (hf\Delta F_{sh}/\eta)(\delta/\sigma_{sh})^2\left|1+(1+2\eta\bar{n}_F\tau/c)^{1/2}\right|. \tag{10}$$

Let us examine the instance when the tracking system band is determined by dynamic error and not by transients. [The ratio θ_m/σ_φ is large or a prediction of the angular velocity $d\theta(t)/dt$ is introduced into the system.] Then it is possible to optimize the tracking system as follows.

We consider that the resultant dynamic and noise errors do not exceed the angle discriminator aperture $\pm\delta$, i.e., $(\sigma_\varphi^2 + \sigma_{sh}^2)^{1/2} \leq \delta/r_0$. Assuming that $\sigma_{sh}^2 = \lambda\sigma_\varphi^2$, we find the minimum value of P_{ave}. Then
$\sigma_m^2(1+1/\lambda) = \delta^2/r_0^2$; $(\delta/\sigma_m)^2 = r_0^2(1+\lambda)/\lambda$; $\sigma_\varphi^2(1+\lambda) = \delta^2/r_0^2$; $\sigma_\varphi^2 = \delta^2/r_0^2(1+\lambda)$.
Using these expressions as well as (8) and (10) for the instances when the background may be neglected, we obtain

$$P_{ave} = \begin{cases} (\pi r_0^4/\eta\beta^2\psi)(\theta_m/\delta)^2 hfF_c(1+\lambda)^2/\lambda & \text{for } m=1; \\ 2(2\sqrt{2}/3)^{1/3}(\pi r_0^{8/3}/\eta\beta^{2/3}\psi)(\theta_m/\delta)^{2/3} hfF_c(1+\lambda)^{4/3}/\lambda & \text{for } m=2; \\ 2\pi\left[\frac{\sin(\pi/2m)}{\sin(5\pi/2m)}\right]^{1/4}\frac{r_0^{5/2}}{\eta\beta^{1/2}\psi}\left(\frac{\theta_m}{\delta}\right)^{1/2} hfF_c\frac{(1+\lambda)^{5/4}}{\lambda} & \text{for } m>2, \end{cases}$$

where δ and δ/r_0 are the required maximum and root-mean-square resultant tracking errors. The minimum values of P_{ave} are reached at $\lambda = 1$ ($m = 1$), $\lambda = 3$ ($m = 2$), $\lambda = 4$ ($m > 2$). Then we finally have

$$P_{ave} = \begin{cases} (4\pi r_0^4/\eta\beta^2\psi)(\theta_m/\delta)^2 hfF_c & \text{for } m=1; \\ \frac{16}{3}\left(\frac{\sqrt{2}}{3}\right)^{1/3}(\pi r_0^{8/3}/\eta\beta^{2/3}\psi)(\theta_m/\delta)^{2/3} hfF_c & \text{for } m=2; \\ \frac{5\pi}{2}\left[\frac{5\sin(\pi/2\pi)}{\sin(5\pi/2m)}\right]^{1/4}\frac{r_0^{5/2}}{\eta\beta^{1/2}\psi}\left(\frac{\theta_m}{\delta}\right)^{1/2} hfF_c & \text{for } m>2. \end{cases}$$

Let us compare the values P_{ave} which were obtained with the necessary optical signal strength P_n at the angle discriminator input for a laser beacon in continuous operating mode. We will determine the value $\mu = P_{ave}/P_n$. For $m \to \infty$, the value of P_n is determined in [3], in this case $\mu = 1.9\beta^{1/2}\psi$. In the general instance it is possible to determine that $\mu = \Delta F_{sh}/\Delta F_{sh.n}$. A graph of the change in μ for $m \to \infty$ is presented in Figure 11.

Let us examine a typical instance when the spectrum of angle flunctuations of the stabilized platform is described by a second order system $\theta(F) = 1/[1 + (F/F_s)^4]$. From Figure 8 we find a tracking system with a continuous signal

$$H(p) = \frac{\varphi(p)}{\theta(p)} = \frac{p^2}{p^2 + kp + k_1 k}; \quad |H(i\omega)|^2 = \frac{\omega^4}{\omega^4 + \omega^2(k^2 - 2k_1 k) + (k_1 k)^2}.$$

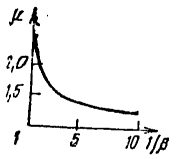

Рис. 11

Figure 11

The amplitude-frequency characteristic of the tracking system is close to the maximly flat characteristic at $k_1 \approx k/2$. Then we obtain $|H(i\omega)|^2 = \omega^4/(\omega^4 + k^4/4)$. The dynamic error is equal to

$$\sigma_\varphi^2 = \int_0^\infty \theta(F)|H(iF)|^2 dF = \int_0^\infty \frac{(2\pi F)^4 dF}{[1 + (F/F_c)^4][(2\pi F)^4 + k^4/4]} = \frac{(\pi F_c^4/2\sqrt{2})(k/2\sqrt{2}\pi - F_c)}{(k/2\sqrt{2}\pi)^4 - F_c^4}.$$

For $k_1 = k/2$ we have $\Delta F_{sh.n} = 3k/8$.

The relative dynamic error is equal to

$$\varepsilon_\varphi^2 = \sigma_\psi^2 \Big/ \int_0^\infty \frac{dF}{1+(F/F_c)^4} = \sigma_\varphi^2 \Big/ \frac{\pi}{2\sqrt{2}} F_c = F_c^2 \frac{4\Delta F_{\text{ш.ш}}/3\sqrt{2\pi} - F_c}{(4\Delta F_{\text{ш.ш}}/3\sqrt{2\pi})^4 - F_c^4}.$$

When the dynamic error is small, $4\Delta F_{\text{ш.ш}}/3\sqrt{2\pi} \gg F_c$, then

$$\Delta F_{\text{ш.ш}} = 3\sqrt{2}\pi F_c / 4\varepsilon_\varphi^{2/3}.$$

Taking the following substitutions into consideration [3]: $\varepsilon_\psi = 4\sigma_\phi / \theta_m$ and $\sigma^2_{\text{ш}} = \lambda\sigma^2_\varphi$ we have

$$P_{\text{ш}} = \frac{2hf}{\eta}\Delta F_{\text{ш.ш}}\left(\frac{\delta}{\sigma_{\text{ш}}}\right)^2 = \frac{2^{1/6}3\pi}{4\eta} F_c^{4/3}\left(\frac{\theta_m}{\delta}\right)^{2/3} hf F_c \frac{(1+\lambda)^{4/3}}{\lambda}.$$

Given an optimum value $\lambda = 3$, we obtain $\mu = 2.3/\beta^{2/3}\psi$.

Let us examine the instance when the background is significantly greater than the quantum noise. Then, from (10)

$$P_{\text{ош}} = \left(\frac{\tau}{T}\right)^{1/2}\frac{hf}{\eta}\left(\frac{\delta}{\sigma_{\text{ш}}}\right)(2\eta\bar{n}_\phi\Delta F_{\text{ш}})^{1/2}.$$

By analogy, for a tracking system with a constant signal, we have

$$P_{\text{ш}} = \frac{hf}{\eta}\left(\frac{\delta}{\sigma_{\text{ш}}}\right)(2\eta\bar{n}_\phi\Delta F_{\text{ш}})^{1/2}.$$

As a result, we obtain $\mu = [(\tau/T)(\Delta F_{\text{ш}}/\Delta F_{\text{ш.ш}})]^{1/2}$. In particular, for $m \to \infty$, $\mu = [(\tau/T)1.9/\beta^{1/2}\psi]^{1/2}$; for $m = 2$, $\mu = [(\tau/T)2.3/\beta^{2/3}\psi]^{1/2}$.

LITERATURE

1. Ward, J. H. EASCON-75 Conf., Washington, USA, 1975.

2. Barry, J. D., et al. Trans. IEEE, 1976, V. COM-24, N 4.

3. Teplyakov, I. M. Paper No. 77-35, XXVIII Congress of the International Astronautical Federation, Prague, Czechoslovakia, 1977.

4. Teplyakov, I. M. Paper No 76-189, XXVII Congress of the International Astronautical Federation, Anaheim, California, USA, 1976; Acta Astronautica, 1979, vol. 6, p 499.

5. "Sovremennaya radiolokatsiya" [Modern Radar] (Trans. from the English), Moscow, Sov. Radio, 1969.

6. Levin, B. R. "Teoreticheskiye osnovy statisticheskoy radiotekniki" [Theoretical Fundamentals of Statistical Radio Engineering], Moscow, Sov. Radio, 1966.

7. Slansky, J. RCA Rev., 1957, vol. 18, No. 2.

8. Beytmen, G.; Erdeyn, A. "Tablitsy integral'nykh preobrazovaniy" "Tables of Integral Transfers] (Translated from the English), Moscow Fizmatgiz, 1969.

9. Gradshteyn, I. S.; Ryzhik, I. M. "Tablitsy integralov, summ, ryadov i proizvedeniy" [Tables of Integrals, Sums, Progressions and Products], Moscow, Fizmatgiz, 1962.

[217-9194]

9194
CSO: 1860

UDC 621.372.823

BASIC PARAMETERS OF BIMETALLIC WAVEGUIDES FOR RADIO-RELAY SYSTEMS OPERATING IN THE 6 GHz RANGE

Moscow ELEKTROSVYAZ' in Russian No 3, 1980 pp 36-38 manuscript received 29 Nov 78

[Article by Yu. I. Isayenko and V. V. Malin]

[Text] The increase in the traffic-handling capacity of radio-relay communications systems makes ever greater demands on the quality of the waveguide line. In connection with this, it has become necessary to develop new (bimetallic, in particular) waveguides that possess considerably higher parameters in comparison with copper waveguides. The design features of circular bimetallic waveguides with a 70-mm internal diameter and the results of an analysis of these waveguides on a transmitting wave H_{11} in the waveguide lines of a radio-relay system in the 4 GHz range are cited in [1].

It is interesting to examine the electrical parameters of bimetallic waveguides in connection with antenna waveguide lines now being introduced into radio-relay nets operating in the 6 GHz range.

Certain questions about the construction of multiwave waveguide lines in the 6 GHz range and, in particular, about those that utilize bimetallic waveguides are analyzed in [2,3].

The utilization of bimetallic waveguides in radio-relay systems of various frequency ranges will provide considerable savings of the copper that is in short supply and will make it possible to consolidate the elements of the antenna waveguide line.

Electrical Parameters.

The ohmic losses of the bimetallic waveguide in the 5.6 to 6.2 GHz frequency band (the working frequency band for systems operating in the 6 GHz range) do not exceed 1.4 dB in a line 100 m long.

The excitation level of the reflected wave H_{11} is calculated according to formulas obtained from the general work equations for a waveguide 70 mm in diameter [4]:

$$\left.\begin{aligned} \overline{W}^{-} &= 0{,}025\,\overline{\delta}_0^2/a^3 + 0{,}11\,\overline{\delta}_2^2/a^3, \\ f &= 5{,}6\ \text{GHz}, \\ \overline{W}^{-} &= 0{,}026\,\overline{\delta}_0^2/a^3 + 0{,}09\,\overline{\delta}_2^2/a^3, \\ f &= 6{,}2\ \text{GHz}. \end{aligned}\right\} \quad (1)$$

The values for $\overline{\delta}_0^2$ and $\overline{\delta}_2^2$ are equal to their values in [1]. The results of the calculations are cited in table 1.

The levels of the wave H_{11}, reflected from the individual junctions, are measured with the aid of a type-IP-6 pulse reflectometer. The levels are less than -60 dB, which corresponds to the calculated data.

The Excitation Level of the Cross-Polarized Wave H_{11}.

The analysis cited in [1] has shown that the level of a cross-polarized wave in a line built up from waveguides with low ellipticity depends upon the angle of rotation of the H_{11} wave's exciter. The highest cross-polarized wave level is obtained with the exciter in the optimum position, if half of the waveguides have the same position for the ellipses and are turned 45° relative to the other half, which have the same position for the ellipses. In this case the amplitude of the cross-polarized wave is

$$A^{\perp} = 0{,}15\left(\frac{\Im z}{\beta_{11}\, a^3}\right)^2, \quad (2)$$

where z is the length of the line, $\beta_{11} = \sqrt{k^2 - \mu_{11}^2/a^2}$, a is the radius of the waveguide, $\mu_{11} = 1.841\ldots$, $k = 2\pi/\lambda$ and $\Im = D_{MAX} - D_{MIN}$. The average ellipticity of the bimetallic waveguide is $\Im \approx 0.04$ mm. The direction of the ellipsis' axes changes along

the axis of the waveguide. In accordance with [1], waveguides with a constant ellipticity approximately equal to 0.02 mm are, from the point of view of the cross-polarized wave, equivalent to those indicated.

With an average line length of 75 m, the highest cross-polarized wave level in accordance with (2) is approximately -35 dB. However, the position of the waveguides in the line is random. For this reason, an estimation of the probability of exceeding the given cross-polarized wave level was carried out according to the method in [1]. Within the limits of -35 to -45 dB the level of the cross-polarized wave can be found with a probability of 0.4 percent. Experimental studies on the line have confirmed the calculations.

1 Тип волны	2 Уровень волн, дБ, на частотах, ГГц	
	5.6	6.2
H_{11}	—79,5	—79,5
E_{01}^{+}	—58	—58
E_{01}^{-}	—61,5	—62
H_{21}^{+}	—57	—56,6
H_{21}^{-}	—72,5	—71
H_{01}^{+}	—55	—55,5
H_{01}^{-}	—62,5	—67
E_{11}^{+}	—69	—71
E_{11}^{-}	—69	—71
H_{31}^{+}	—	—83,5
H_{31}^{-}	—	—83,3

Table 1

1 - Type of wave; 2 - Level of wave, dB, at frequency, GHz

1 Тип паразитной волны	2 f, ГГц	B_0	B_1	B_2	B_3
E_{01}^{+}	5,6 6,2	0 0	0,29 0,27	0 0	2,46 3,03
E_{01}^{-}	5,6 6,2	0 0	0,29 0,27	0 0	0,0058 0,0042
H_{21}^{+}	5,6 6,2	0 0	0,74 0,75	0 0	0,87 1,20
H_{21}^{-}	5,6 6,2	0 0	0,024 0,035	0 0	0,00056 0,00060
H_{01}^{+}	5,6 6,2	0 0	1,3 1,2	0 0	0,28 0,40
H_{01}^{-}	5,6 6,2	0 0	0,25 0,08	0 0	0,0094 0,0018
E_{11}^{+}	5,6 6,2	0,33 0,20	0 0	0,33 0,21	0 0
E_{11}^{-}	5,6 6,2	0,33 0,20	0 0	0,33 0,21	0 0
H_{31}^{+}	5,6 6,2	— 0	— 0	— 0,11	— 0
H_{31}^{-}	5,6 6,2	— 0	— 0	— 0,027	— 0

Table 2

1 - Type of parasitic wave; 2 - Frequency, GHz

In this manner, the method of assembling lines cited in [1] can also be applied in the 6 GHz range. The application of precision waveguides makes it possible to obtain a cross-polarized wave level not lower than -35 to -40 dB. The measurements that have been carried out have shown that a line tuned to the 4 GHz range keeps its high parameters when switched to the 6 GHz range by rotating only the exciter of H_{11}.

The Excitation Level of Parasitic Waves.

Parasitic waves E_{01}, H_{21}, H_{01}, E_{11} and H_{31} can propagate in the waveguide in the 6 GHz range. We will examine the basic non-uniformities of the waveguide and the parasitic waves they excite.

A non-uniformity in the diameters of the waveguide ends leads to an excitation of direct and reverse waves E_{11} at the butt junction, while ellipticity of the waveguide's ends leads to the excitation of direct and reverse waves E_{11} and H_{31}. The radial displacement, deflection and curvature of the waveguide axes at the junction lead to an excitation of direct and reverse waves E_{01}, H_{21} and H_{01}. The fluctuation in the diameter along the axis of the waveguide generates direct and reverse waves E_{11} and H_{31}.

Calculation of the Levels of Parasitic Waves Excited on the Waveguide Non-Uniformities. Butt Junctions.

The theoretical estimation of the average energy ($\overline{W}$) of parasitic waves excited at one butt junction was carried out according to a formula obtained from the general equations [4] for a waveguide 70 mm in diameter:

$$\overline{W}^{\pm} = B_0 \overline{\delta_0^2}/a^2 + B_1 \overline{\delta_1^2}/a^2 + B_2 \overline{\delta_2^2}/a^2 + B_3 \overline{\theta^2}, \quad (3)$$

where $\overline{\delta_0^2}$, $\overline{\delta_1^2}$ and $\overline{\delta_2^2}$ are the average values for the squares of the amplitudes of the zero, first and second harmonics of the Fourier series function $\delta(\varphi)$ characterizing the step in the first junction; $\overline{\theta^2}$ is the average value for the square of the axis deflection angle in the joined waveguides. Values for the coefficients B_j are cited in table 2 for two frequency values. The fact that certain of the coefficients are equal to zero means that the corresponding harmonic does not take part in exciting the given type of parasitic wave. The "+" index pertains to the direct parasitic wave, while "-" applies to the reverse parasitic wave.

As a result of a statistical analysis of the measurements of the waveguide ends, we obtained:

$$\sqrt{\overline{\delta_0^2}} = 0{,}01 \text{ мм}; \sqrt{\overline{\delta_1^2}} = 0{,}08 \text{ мм}; \sqrt{\overline{\delta_2^2}} = 0{,}02 \text{ мм}; \sqrt{\overline{\theta^2}} = 0{,}0008 \text{ rad}.$$

The results of a calculation according to (3) are cited in table 1.

For a waveguide line with n butt junctions, the average value for the energy of the resultant reflected wave or the resultant parasitic wave is n times greater than for one junction.

Gradually Sloping Waveguide Non-Uniformities.

As the analysis has shown, the non-uniformities are the deflection of the waveguide axis, the fluctuation in the diameter and

the variable ellipticity. The amplitudes of the direct parasitic waves at the output of a waveguide of length L according to [4] are:

$$A_j = e^{-i\beta_j L} F_{11,j} \times$$

$$\times \int_0^L l(z)\, e^{-i(\beta_{11}-\beta_j)z}\, dz, \qquad (4)$$

where $l(z)$ is the function characterizing the non-uniformity: for a waveguide with a deflected axis $l(z)=x(z)$ [$x(z)$ is the curve of the axis]; for a waveguide of fluctuating diameter

$$l(z) = \frac{1}{2a} \frac{dD(z)}{dz}$$

($D(z)$ is the diameter); for a waveguide with fluctuating ellipticity

$$l(z) = \frac{1}{4a} \frac{d\vartheta(z)}{dz}$$

($\vartheta(z)$ is the ellipticity); $F_{11,j}$ are the so-called coupling factors. The general equations for them are given in [4]. In table 3 the values for the chief parameters of formula (4) are cited.

Values for the curve of the axis $x(z)$, the fluctuation in the diameter $D(z)$ and the fluctuations in ellipticity $\vartheta(z)$ which are necessary for the calculation according to (4) were measured for a set of waveguides with the help of specially developed equipment. As a result of the calculations, the following average values (for the set of waveguides and for the range of frequencies) of the wave levels have been obtained for a single waveguide 5 m in length: $E_{01} \approx -55$ dB, $H_{01} \approx -64$ dB, $H_{21} \approx -53$ dB, $E_{11} \approx -66$ dB and $H_{31} \approx -70$ dB. For a waveguide line consisting of n waveguides, the average value for the energy of the resultant parasitic wave is n times greater than in a single waveguide. The levels of the reverse waves, as the analysis has shown, are considerably less than those of the direct waves and therefore are not conducted.

In a line 100 m long, the average level (taking into account the non-uniformity in the butt junction and the gradually sloping non-uniformities) of the waves comprises: E_{01} of approximately -40 dB; H_{21} of -38.5 dB; H_{01} of -41.5 dB; E_{11} of -51.5 dB; and H_{31} of -57 dB.

1 Тип волны	2 Тип неоднородности	3 f, ГГц	$\beta_{11}-\beta_{j}$, 1/см	$F_{11,\ j}$
E_{01}	4 Кривизна оси	5,6 6,2	0,0977 0,0853	1 1,570 1 1,740
H_{11}	5 То же	5,6 6,2	0,265 0,226	1 3,268 1 3,863
H_{01}	6 То же	5,6 6,2	0,627 0,489	1 0,522 1 0,628
E_{11}	7 Пульсация диаметра	5,6 6,2	0,627 0,489	0,571 0,417
E_{11}	8 Переменная эллиптичность	5,6 6,2	0,627 0,489	0,571 0,471
H_{21}	9 То же	5,6 6,2	— 0,692	— 0,330

Table 3

1 - Type of wave; 2 - Type of non-uniformity; 3 - Frequency, GHz; 4 - Curvature of axis; 5 - Same; 6 - Same; 7 - Fluctuation in the diameter; 8 - Varying ellipticity; 9 - Same.

The values obtained for the cross-polarized wave levels, the reflected wave H_{11} and all the parasitic waves for a bimetallic waveguide line show that bimetallic waveguides in both the 6 and 4 GHz ranges possess very high electrical parameters.

Bimetallic waveguides in combination with other waveguide elements with improved parameters were tested in the experimental section of the "Kurs-6"* radio-relay system. As a result, they were able to insure (from the point of view of introduced noise) a traffic-handling capacity for the radio-relay system of more than 1320 audio frequency channels.

Conclusions.

1. The bimetallic waveguides 70 m in diameter and up to 120 m in overall length that have been developed and put into production provide for the organization of more than 1320 audio frequency channels in the 6 GHz range when the "Kurs-6" equipment is utilized.

* Research in the experimental section was conducted under the guidance of B. S. Nadanenko.

2. Bimetallic waveguides may be employed as unifying elements in long waveguide lines with small losses in the 4 and 6 GHz ranges.

3. Mixed waveguide lines for the simultaneous transmission of signals in the 4 and 6 GHz ranges may be constructed on the basis of bimetallic waveguides.

BIBLIOGRAPHY

1. Isayenko, Yu. M., Malin, V. V. and Kokonin, A. P. "Bimetallic Circular Waveguides for Radio-Relay Lines," ELEKTROSVYAZ', No 9, 1978.

2. Nadanenko, B. S. and Tartakovskiy, L. S. "Transient Noise in Waveguide Lines of Radio-Relay Trunks," ELEKTROSVYAZ', No 1, 1973.

3. Nadanenko, B. S., Khrichevskiy, V. N. and Polushin, G. P. "The Application of Multimode Waveguide Sections in Radio-Relay Systems," Proceedings of the Fifth Colloquium on Microwave Communications," Budapest, 24-30 Jun 74.

4. Katsenelenbaum, B. Z. "Teoriya neregulyarnykh volnovodov s medlenno menyayushchimisya parametrami," [Theory of Non-Regular Waveguides With Slowly Varying Parameters], Moscow, AN SSSR, 1961.

[222-9512]

9512
CSO: 1860

UDC 621.376.56

IKM-15 RURAL COMMUNICATIONS EQUIPMENT

Moscow ELEKTROSVYAZ' in Russian No 3, Mar 80 pp 1-7 manuscript received 2 Jul 79

[Article by Yu. A. Alekseyev, I. A. Lozovoy, P. V. Mel'nikov, V. F. Myagkov and L. A. Chernyshev]

[Text] The development of digital technology for the transmission of telephone communications has proceeded by means of the utilization of 32 channel intervals in pulse-code modulated (PCM) transmission systems possessing a transmission rate of 2048K bits/sec, and the utilization of a 13-segment coder with a non-linear logarithmic response of the type A=87.6. These basic principles have received wide dissemination, and the International Consultative Committee on Telegraphy and Telephony (CCITT) has formulated a number of recommendations regulating the characteristics of the telephone channels, the structure of the cycle and other parameters of equipment with PCM. The IKM-30 equipment (possessing a transmission rate of 2048K bits/sec and satisfying the recommendations of the CCITT) as well as a number of other higher-order transmission systems, for example, the IKM-120, have been put into production in recent years both in our country and abroad.

At the present time, IKM-12M equipment is being employed in rural exchanges for the organization of trunk lines between stations. This equipment does not link up well with broadcast system equipment built on the basis of the IKM-30. Moreover, the 7-bit coding used in the IKM-12M does not insure the necessary transmission quality of telephone signals when there are a great many retransmissions and repeat PCM conversions. Therefore, instead of modernizing the IKM-12M equipment, a decision was made to develop the IKM-15 15-channel PCM transmission system. It possesses characteristics that are more suitable for link-up with higher-order transmission systems--the IKM-30, IKM-120, etc.

Modern integrated circuits and a number of technical and design solutions which insure high adaptability for industrial production have been employed in the development of the apparatus. Commercial production of the IKM-15 equipment is planned for 1980.

Purpose.

The IKM-15 15-channel PCM transmission system is intended for the organization of interoffice trunks between rural two-motion selector or crossbar-type automatic exchanges along KSPP 1x4x0.9 or KSPP 1x4x1.2 cables or along a VTSP [further expansion not provided]. The IKM-15 equipment makes it possible to organize: 15 audio-frequency channels; from 15 to 45 remote signal channels; four 100-baud or two 200-baud telegraph channels; or one second-class broadcast channel instead of two audio-frequency channels. Besides the interoffice trunks, lines are made available to the exchange's rural subscribers, which connect them to the automatic district exchange, bypassing the terminal station. A subscriber's set in the IKM-15 equipment is utilized for this.

There is a telegraph matching unit in the IKM-15 equipment used for the organization of telegraph channels. This unit converts the telegraph impulses that arrive at its input into signals that are suitable for input into the equipment's distribution circuit.

The IKM-15's broadcast channel is organized by replacing the individual equipment for the two audio frequencies with equipment for the broadcast channel. The broadcast channel is a duplex channel. The direction opposite the transmission of the of the broadcast channel is used for monitoring the transmission quality.

Instead of one audio-frequency channel, it is feasible to organize in the IKM-15 equipment a 64K bits/sec digital data transmission channel whose parameters correspond to the CCITT's recommendation G. 732. Furthermore, provisions have been made for the feasibility of working with electronic matching units (SU-IKM) which in the future will replace the relay assemblies of the trunk relays that belong to the automatic exchange. In this case, each audio-frequency channel will be given three signal channels.

The IKM-15 equipment insures transmission along the line at the rate of 1024K bits/sec. Two such signals may be combined into one common stream at a rate of 2048K bits/sec, or eight IKM-15 signals at a rate of 8448K bits/sec. This corresponds to the accepted standards for the IKM-120 equipment.

The characteristics of the coders in the IKM-15 and IKM-30 equipment are identical. Therefore, it is possible to connect two IKM-15 outputs in order that a standard IKM-30 may be installed at the opposite end of the line. IKM-15x2 and IKM-15x8 connecting equipment is now being made on the basis of the IKM-15. It will be able to interact directly with the IKM-30 and IKM-120 units.

Technical Specifications.

The transmission rate for a digital signal at the output of a terminal station is 1024K bits/sec. The equipment's range is 50 km, but with the application of serviced stations the range increases to 100 km. The maximum distance between intermediate stations for KSPP 1x4x0.9 cable is 7.2 km and 7.4 km for KSPP 1x4x1.2 cable. The intermediate station's regenerative repeaters are equipped with compensation amplifiers that have automatic gain control and automatically retune when there is a change in the length of the regeneration segments: from 4 to 7.5 km for KSPP 1x4x0.9 cable and from 4.7 to 7.4 km for KSPP 1x4x1.2 cable. In this case, the attenuation in the regeneration segment is within the limits of 26 to 46 dB.

Loudspeaker service communications are organized through a phantom circuit between terminal stations as well as between a terminal station and any intermediate station. Its range without intermediate amplification is up to 50 km.

The signal formed at the terminal station for transmission into the line has the form of a rectangular pulse with an amplitude of 3 B and a duration equal to the time interval t_i=0.98 μsec (fig. 2).

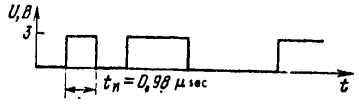

Fig. 1

The IKM-15 equipment is built according to the principle of time-division allocation of the channels, and therefore one of its characteristics is the time spectrum, which is the sequence of time intervals combined into the channel intervals and cycles (fig. 2).

The cycles with a duration of 125 μsec follow one after another at a frequency that is equal to an 8 kHz discrete frequency. Each cycle contains 16 channel intervals 0-15, and each channel interval consists of eight timing intervals. There are 128

timing intervals in all in the cycle. The channel intervals from the first to the fifteenth contain information relating to the corresponding audio-frequency channels. The information in these channel intervals is registered in the form of 8-bit binary-coded combinations P1-P8.

Channel interval 0 is intended for the transmission of synchronous signals serving to determine the beginning of the cycles and the supercycles, as well as for the transmission of information coming from the signal channels [channels for the transmission of control and interaction signals of the automatic telephone exchange] and telegraph channels. The signal of the cyclic synchronization is registered in the form of the fixed combination 110 in the time intervals 6-8.

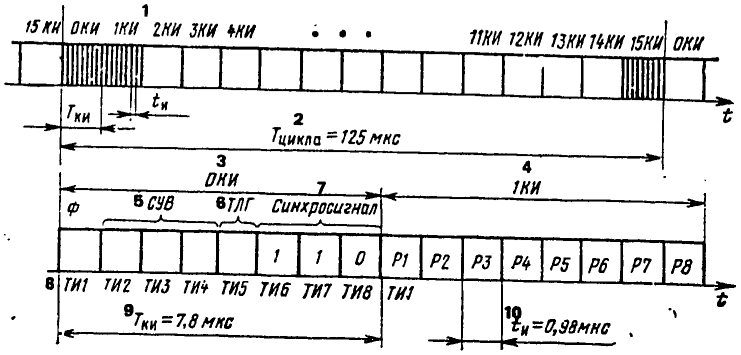

Fig. 2

1 - Channel intervals 0-15; 2 - Time of cycle 125 μsec; 3 - Channel interval 0; 4 - Channel interval 1; 5 - Control and interaction signal; 6 - Telegraph; 7 - Synchrosignal; 8 - Time intervals 1-8; 9 - Time interval T_i = 7.8 μsec; 10 - Time interval t_i = 0.98 μsec.

A supercycle is formed by 16 consecutive cycles. In timing interval 1, channel interval 0, a supercycle synchronization signal is transmitted at the beginning of each supercycle. That signal insures the proper distribution of information along the control and interaction signal channels upon reception.

In accordance with the principle of time division of channels, the information that comes from the control and interaction channels is registered in time intervals 2-4 of all 16 successive cycles: in time interval 2 is registered the informa-

tion from the 16 channels of the first group; in time interval 3 is information from the second group; and in time interval 4 is information from the third group.

Information arriving from the telegraph channels is registered in time interval 5, channel interval 0. The basic audio frequency channel parameters of the IKM-15 equipment satisfy the standards of recommendation G. 712: the input and output levels of the audio-frequency channels are -13 and +4.3 dB, respectively; the gain of the audio-frequency channels is set with an accuracy of ±0.3 dB, and the stability of the gain over the course of a month is ±0.5 dB; the amplitude-frequency response of the overall line attenuation a of the channel is laid out in the scale depicted in fig. 3a--the amplitude-frequency response norm corresponds to 1/5 the CCITT's norm for the audio-frequency channel; the immunity from total pulse modulation distortion (the S/N ratio) as a function of the relative level of the input signal r is not less than the values in the scale in fig. 3b; the level of weighted noise in the open channel does not exceed 500 pW at the zero reference level; the immunity from audible crosstalk is not less than 65 dB.

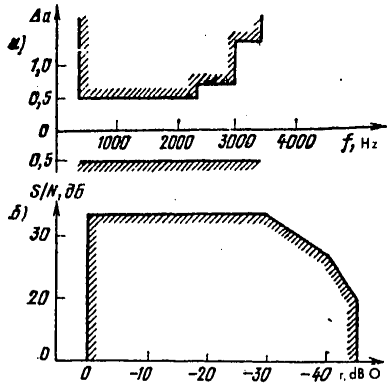

Fig. 3

Power supply to the IKM-15 equipment is accomplished through a power source common to the automatic exchange with a voltage of 60 V, +20/-10 percent. The remote supply for the intermediate station is carried out by means of a phantom circuit from one

terminal station. At each intermediate station and terminal station feeding the line from opposite ends, loop equipment is installed. It is controlled by means of reversing the current from the remote supply. The power requirement for a line of maximum length does not exceed 180 W.

The block diagram of the IKM-15 equipment is depicted in fig. 4. The apparatus consists of terminal stations 1 and 2 and the line equipment.

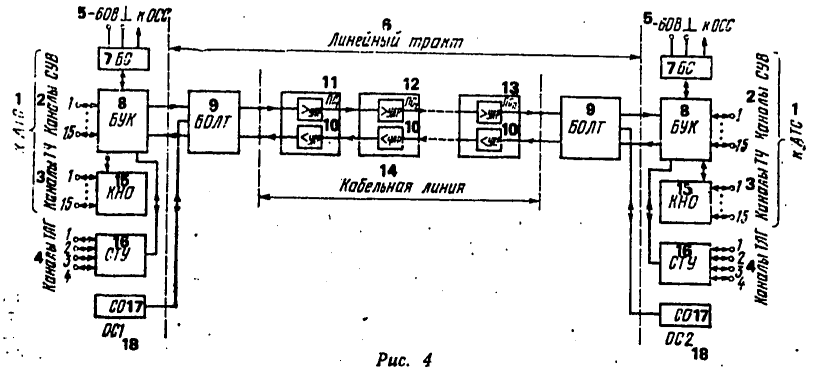

Рис. 4

1 - To automatic telephone exchange; 2 - Control and interaction signal channels; 3 - Audio-frequency channels; 4 - Telegraph channels; 5 - Minus 60 V to general station alarm signal unit; 6 - Line circuit; 7 - Alarm unit; 8 - Multiplexing and encoding unit; 9 - Line terminal unit; 10 - Line regenerative amplifiers; 11 - Intermediate station 1; 12 - Intermediate station 2; 13 - Intermediate station 3; 14 - Cable line; 15 - Low-frequency terminal unit; 16 - Matching telegraph unit; 17 - Service equipment; 18 - Terminal stations 1 and 2.

Each terminal station consists of:

--an alarm unit which insures the power supply to the terminal station and provides the alarm when there is a breakdown in any of the terminal station's units. The alarm signal is then transmitted to common and general station alarm signal units;

--a multiplexing and encoding unit intended for time division and distribution of the channels as well as the analog-to-digital conversion (encoding) of the audio-frequency signals;

--a low-frequency terminal unit assembly containing 15 low-frequency terminal units which, when the connections are made between the channels of the IKM-15 equipment and the automatic exchange units, convert the four-lead channel terminals with levels of -13 and +4.3 dB at the input and the output into two-lead terminals with levels of 0 and 7 dB or 0 and 3.5 dB. Furthermore, on signal from the trunk exchange, the units provide for automatic tandem switching into a four-lead mode with levels of -3.5 and -3.5 dB (low-frequency terminal unit II) or into the two-lead mode with levels of 0 and -3.5 dB (low-frequency terminal unit I);

--a block of matching telegraph units which provide for the match-up of telegraph signals with the IKM-15's digital information transmission channel;

--a service equipment block which serves for the organization of service communications on the phantom circuit and which contains the intercommunications equipment for communicating on the telephone channels, as well as switching equipment for monitoring the audio-frequency and control and interaction signal channels.

The line equipment consists of:

--a line terminal unit intended for the regeneration of of the digital signal taken from the station section of the cable line, for the remote power supply of the line regenerators, for the reception of voice-frequency service calls, for the lead-in of cable and for protection from dangerous voltages. The line terminal unit is made in two configurations: the first contains a remote power-supply unit, while the second, instead of the remote power-supply unit, contains a remote loop that makes it possible to form the circuit of the terminal station;

--intermediate stations, each containing two line regeneration amplifiers (one for each direction of transmission) for the regeneration of digital signals transmitted along the cable line; the line regeneration amplifier in the IKM-15 contains an amplifier with an automatic compensator and automatic level control, which make it possible to connect the intermediate stations into the line without worrying about the length of the regeneration segments (within the limits of the standards cited above). In addition, further attenuation of the regeneration segment to the nominal level through a collection of phantom circuits is not required.

The audio-frequency signals from the automatic exchange's subscribers arrive at the low-frequency terminal unit of terminal station 1. The low-frequency terminal unit's outputs are con-

nected with the four-lead terminals of the multiplexing and encoding unit. The encoded binary combinations that correspond to the instantaneous values of the telephone signals leave the output of the multiplexing and encoding unit and arrive at the line through the line terminal unit. The binary digital signal passing down the line is regenerated at each intermediate station. At each following regeneration segment the signal is transmitted in exactly the same form it had at the output of the multiplexing and encoding unit. While passing through the last regeneration segment, the binary signal is restored by the final regenerator of the line terminal unit, and a signal analogous in form to that at the output of terminal station 1 is received at the input of the multiplexing and encoding unit of terminal station 2.

A reverse transformation of the signals takes place in the multiplexing and encoding unit--from digital to analog form--and the signals are distributed on the audio-frequency channels. The telephone signals from the output of the multiplexing and encoding unit are sent to the subscribers of the automatic exchange through the low-frequency terminal unit. The control and interaction signals for the automatic exchange arrive at the multiplexing and encoding unit through the control and interaction signal channels.

Signals from the telegraph sets arrive at the inputs of the matching telegraph unit block which is connected to the multiplexing and encoding unit through reception and transmission circuits.

The block diagram of the multiplexing and encoding unit is represented in fig. 5. The audio-frequency signals arrive at the inputs of the low-frequency filters F1-F15. These filters impede the components that are outside the range of audio frequencies. From the filter outputs the signals proceed to the keys of modulators M1-M15 which then form pulse-amplitude modulated (PAM) signals consisting of pulses with a 3 μsec duration and a reception frequency of 8 kHz.

Each of the 15 switches M1-M15 operates at various moments in time, shifted 7.81 μsec relative to the adjacent channels. The outputs of all the keys are joined together, and, thus, all the individual PAM signals operating at various channel intervals of time are united in a group PAM signal. The group PAM signal arrives at the input of the No 1 amplifier which charges capacitor C. Capacitor C insures the formation of a flat crest on each PAM signal arriving at amplifier 2.

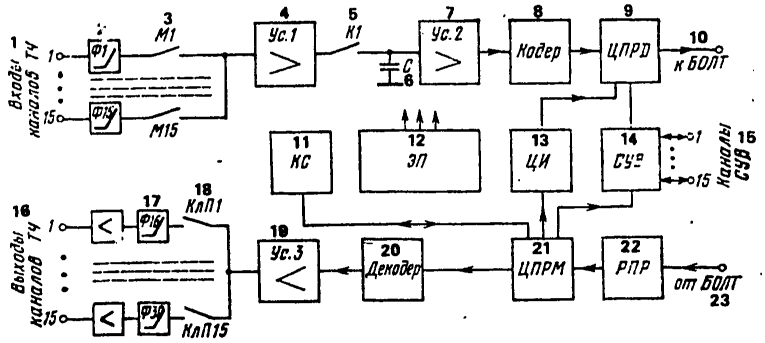

Fig. 5

1 - Inputs of the audio-frequency channels; 2 - Filters F1-F15; 3 - Modulators M1-M15; 4 - Amplifier 1; 5 - Key 1; 6 - Capacitor C; 7 - Amplifier 2; 8 - Encoder; 9 - TsPRD [digital signal transmission]; 10 - To line terminal unit; 11 - Alarm control unit; 12 - Power supply; 13 - Digital data; 14 - Control and interaction signal unit; 15 - Control and interaction signal channels; 16 - Audio-frequency channel outputs; 17 - Filters F16-F30; 18 - Reception keys 1-15; 19 - Amplifier 3; 20 - Decoder; 21 - TsPRM [expansion not provided]; 22 - Reception regenerator; 23 - From line terminal unit.

The signal from the output of amplifier 2 proceeds to the coder input. The coder digitally converts an infinite set of amplitudes of the PAM-signal pulses into a sequence of eight-bit binary-coded combinations. During operation, the coder measures the amplitude of the arriving PAM signal. The result of the measurement of this amplitude is presented in the form of an encoded combination that corresponds to a certain small range of amplitudes--to the so-called quantization interval--within whose limits the arriving PAM signal appears. The encoded combinations appear at the output of the coder in the form of a binary digital signal.

The IKM-15's coder performs a non-uniform quantization of the input signals. The law of quantization interval variation (the compressor response) is given by line-segmented curve 2 in fig. 6, which consists of 16 segments: eight are for the positive values of x and eight are for the negative. The compressor curve for $0 \leq x \leq 1$ is shown in fig. 6.

As can be seen in fig. 6, the quantization intervals within the limits of the first segment 1C are equal to $\Delta_1=1/32$; within the limits of the second segment $\Delta_2=1/64$. In each successive segment the quantization intervals decrease by one half: $\Delta_3=1/128$, $\Delta_4=1/256$, $\Delta_5=1/512$, $\Delta_6=1/1024$, $\Delta_7=\Delta_8=1/2048$. The seventh and eighth segments have the same slope and dimensions (fig. 6a). Upon examination of the overall compressor curve (fig. 6a), four segments in the center of the curve form a section of straight line. This section is frequently called a single segment. When this allowance is made, the curve has 13 segments. The 13-segment broken curve approximates logarithmic curve 1 (fig. 6) with a rectilinear initial segment. The analytic expression for curve 1 is:

$$\begin{cases} y=\dfrac{Ax}{1+\ln A} & 0\leqslant x\leqslant\dfrac{1}{A}; \\ y=\dfrac{1+\ln Ax}{1+\ln A} & \dfrac{1}{A}\leqslant x\leqslant 1, \end{cases}$$

where $A=87{,}6$.

The binary signal from the coder's output arrives at the digital transmission signal processor (TsPRD) (see fig. 5), which varies the signal's statistical characteristics. Digital binary signals from the digital data unit and the control and interaction signal unit also arrive at the input of the digital transmission signal processor. These signals contain information from the telegraph channels and the remote signal channels, respectively. Signals from the digital data and control and interaction signal units are included in the group signal until it is processed. After the group signal is processed in the digital transmission signal processor, the synchrocombination 110 is introduced into it. The group signal from from the digital transmission signal processor arrives at the line through the line terminal unit. The group signal from the line, having passed the line terminal unit, arrives at the input of the compression and encoding unit's receiving unit. The receiving generator at whose input the signal arrives is a simplified regenerator without an amplifier. It separates the timing frequency from the signal and forms it into a pulsed time sequence with a frequency of 1024 kHz. This sequence is necessary for the operation of the receiving station's generator equipment. The group signal from the receiving regenerator

arrives at the TsPRM unit which carries out: the synchronization of the receiving station by means of a synchrosignal; reverse processing of the group signal; and the separation of the digital signals for the decoder, the digital data unit and the control and interaction signal unit. The digital data and control and interaction signal units direct the telegraph signals and the control and interaction signals to the outputs of the corresponding channels.

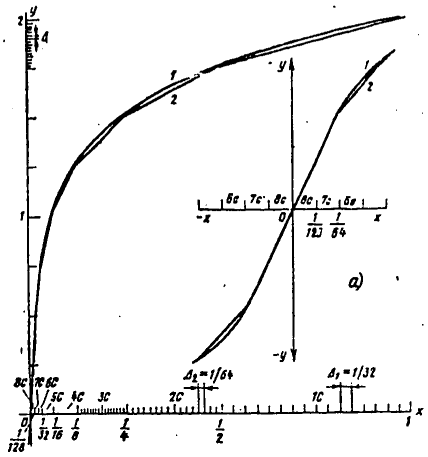

Fig. 6

The digital signal arrives at the input of the decoder. Each coded combination causes a pulse to appear at the decoder's output. This pulse possesses an amplitude very close to the amplitude of the signal changed by the coder. As a result, a group PAM signal corresponding to the group PAM signal at the input of the coder appears at the decoder's output. Having passed through amplifier 3, the PAM signal arrives at receiver keys 1-15, which carry out time division of the group PAM signal on individual circuits with the help of command impulses. These impulses close the receiver keys in turn at those moments in time when a pulse destined for the engaged individual circuit appears at the output of amplifier 3. The individual circuits contain LF filters (F16-F30) and amplifiers from whose outputs the audio-frequency signals then reach the subscribers.

Contained within the multiplexing and encoding unit is an alarm control unit which monitors the operation of the IKM-15 and sends out an alarm when there are breakdowns of various line segments. The multiplexing and encoding unit also contains power-supply equipment which provides the multiplexing and encoding unit assemblies with the nominal voltage required for operations.

The block diagram of the line terminal unit is depicted in fig. 7. The line cable leads to the cable input assembly of the line terminal unit. The cable input assembly provides all units of the terminal's equipment with protection from dangerous voltages induced in the line. The central points of the line windings of the transformers form a phantom circuit to which the remote power-supply or remote-loop devices are connected. The voice-frequency ringing set and the service communications input-output are likewise connected to the phantom circuit.

The signal from the multiplexing and encoding unit passes immediately to the unit's line transformer and farther on is directed into the line. The signal from the station segment of the line is directed through the multiplexing and encoding unit to the input of the terminal regenerator, which restores the signal. A binary group signal from the output of the terminal regenerator proceeds to the input of the receiver portion of the multiplexing and encoding unit.

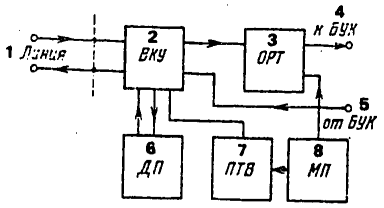

Fig. 7

1 - Line; 2 - Cable input assembly; 3 - Terminal regenerator; 4 - To multiplexing and encoding unit; 5 - From multiplexing and encoding unit; 6 - Remote power supply; 7 - Voice frequency ringing set; 8 - Local power supply.

The remote power supply insures that direct current arrives at the phantom circuit to supply the regenerators at the intermediate stations. At the station opposite the remote power supply a remote circuit is installed in the line terminal unit.

The current from the remote power supply then flows through this remote circuit unit. The remote circuit carries out remote switching of the terminal station's circuit on a signal from the opposite terminal station. The line terminal unit also includes a local power supply unit which powers the assemblies of the line terminal unit.

Design and Assembly.

The elements of the IKM-15 are designed so that they can be mounted in an angle-bar rack up to 2600 mm in height. The width of the rack center-to-center at the mounting holes is 600 mm. An example of the elements' arrangement in the rack is presented in fig. 8.

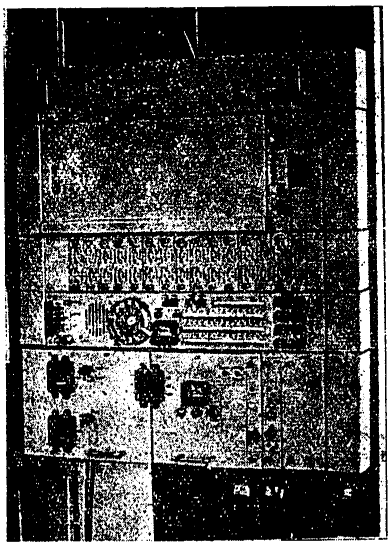

8

The equipment units consist of elements connected to the units by plug connectors. The units are likewise fitted with plug connectors which serve as alignment guides. By virtue of these plug connectors, a damaged unit (or element) can easily be removed and replaced with one in good working order. Provisions have been made for different element and unit connections, dependent upon the operating conditions. The IKM-15's

terminal station has 12 unit configurations, depending upon its purpose: for operating two-motion selector or crossbar-type automatic exchanges with or without a broadcast channel; with electronic matching devices or with the organization of telegraph channels.

The line equipment provides for two versions of the line terminal unit and for varying numbers of intermediate stations: depending upon the length of the line, the number of intermediate stations may vary from one to seven.

The equipment also includes so-called "expansion sets" which are collections of various elements. These make it possible to build up the terminal station's rack-mounted equipment to four sets and to build up the intermediate station's regenerators to two sets.

Operation of the IKM-15 Equipment.

No adjustments are required during the installation and operation of the IKM-15 equipment. When designing and preparing the line for operation it is necessary to certify the line and the terminal equipment. For this, a line set is used which consists of a telephone call set that operates on the phantom circuit and a universal line measurement instrument that insures the measurement of attenuation in the cable and the measurement of transients at a frequency of 512 kHz. When the line is certified with the aid of the universal line measurement instrument, the interference immunity of the regenerators is also checked. The universal line measurement instrument provides for the same measurements at frequencies of 352 and 1024 kHz for the IKM-12M and IKM-30 installations.

Routine maintenance checks on the condition of the line should be carried out once each year. During operation, checks on the function of the trunk lines are carried out on the side of the automatic exchange's instruments with the same frequency that they are carried out during the operation of the automatic telephone exchange.

The certification and routine maintenance checks on the IKM-15 terminal equipment are carried out with the help of a PEI-1 performance measurement instrument which makes it possible to measure the basic characteristics of the audio-frequency channels: the overall line attenuation, immunity from quantization distortion and crosstalk between channels.

The installation's service equipment makes it possible to sequentially switch all the channels over to jacks, to which are connected the measurement instruments or telephone call sets

that form a part of the service equipment. The service equipment block makes it possible to check the installation's signal channels with the help of an automatic telephone dial and a switching unit.

Equipment repair is accomplished by replacing the malfunctioning units with serviceable units from the spare part, instrument and accessory kit. The malfunctioning units taken from the line are repaired in special equipment laboratories. The determination of the malfunctioning unit is accomplished from the terminal station with the aid of circuits which can be set up automatically from the station with remote power-supply equipment.

Test operations of the IKM-15 installation have shown both high reliability for the equipment and stability for its parameters during operation as well as its conformity to the requirements of the CCITT.

BIBLIOGRAPHY

1. Polyaka, M.U.,ed. "Apparatura uplotneniya IKM-12M dlya sel'skoy svyazi" [IKM-12M Multiplexing Equipment for Rural Communications], Moscow, Svyaz', 1976.

2. Gurevich, V. E., Lopushnyan, Yu. G. and Rabinovich, G. V. "Impul'sno-kodovaya modulyatsiya v mnogokanal'noy svyazi" [Pulse-Code Modulation in Multichannel Communications], Moscow, Svyaz', 1973.

3. Lopushnyan, Yu. G., et al. "IKM-30 Equipment for the Multiplexing of Urban Telephone Cables," ELEKTROSVYAZ', No 2, 1977.

[222-9512]

9512
CSO: 1860

UDC 621.395.34

RSL-DSh-ATS INTERSTATION COMMUNICATIONS EQUIPMENT FOR RURAL TELEPHONE EXCHANGES

Moscow ELEKTROSVYAZ' in Russian No 3, 1980 pp 13-15 manuscript received 18 May 77

[Article by L. A. Berezovich and L. M. Brener]

[Text] During the 1960's, the two-motion selector ATS-100/500 (100/500M) units were widely used in rural telephone exchanges (RTE's). In order to incorporate the physical trunk lines into the ATS-100/500 equipment, there were inductive sets in the trunk relay which were also suitable for incorporating the transmission system's high-frequency channels. The sets possessed considerable shortcomings, chief among which were: the lack of a signal with which to hold the opposite automatic exchange, which is not acceptable for the two-way use of lines and channels, particularly when the terminal stations and tandem exchanges are unattended; the absence of a signal with which to monitor the channel's serviceability; inadequate immunity from pulse-type noise; the impossibility of joint operations with local communications equipment, that is, upon automation of the trunk exchange.

In order to eliminate the shortcomings listed and to reduce operational expenditures for servicing interstation communications in the rural exchange, new trunk relay sets have been developed for rural automatic exchanges of the crossbar or two-motion selector systems.

The Leningrad branch of the Central Scientific Research Institute for Communications in conjunction with the Sverdlovsk affiliate of the Central Design Bureau has developed trunk relay-two motion selector-automatic telephone exchange (RSL-DSh-ATS) equipment which incorporates trunk relay sets for two-motion selector automatic exchanges. The trunk relay sets included in the RSL-DSh-ATS equipment are designed for operations along physical interstation lines as well as along the rural

telephone exchange's HF transmission channels with a signal channel outside the voice-frequency band. These sets make it possible to establish terminal and through connections in the presence of AON [automatic number identification] equipment at the stations and without it. These sets operate in conjunction with similar assemblies of the two-motion selector and crossbar automatic exchanges and can operate with the old-type sets until the district trunk exchange is fully automated. Thus, the principle of continuity is maintained and the feasibility of gradually replacing the switching equipment in the rural district is insured. The RSL-DSh-ATS racks are universal and make it possible to accomodate both inductive and voice sets; they can be mounted on the floor as well as in standard metal racks of two-motion selector automatic exchanges instead of the old trunk relay racks.

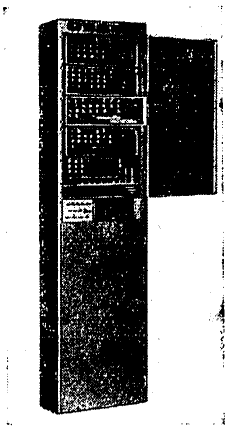

1

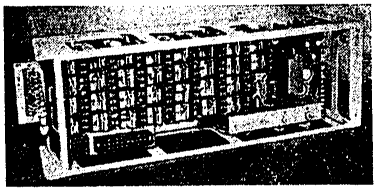

2

The RSL-DSh-ATS equipment contains: the RSL-DSh-ATS rack (fig. 1) with two G-2600-K generators and signalling devices; a mounting plate for the RSLI-D [further expansion not provided] set (fig. 2); a voice set mounting plate RSLUT-D (fig. 3) with a P-2600-2 receiver; and a PP-RSL control panel with movable cart (fig. 4). The technical data for the component parts of the equipment are cited in table 1.

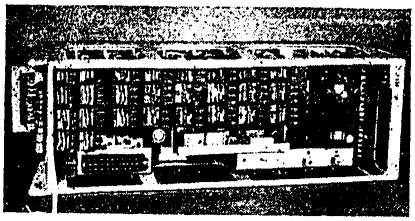

3

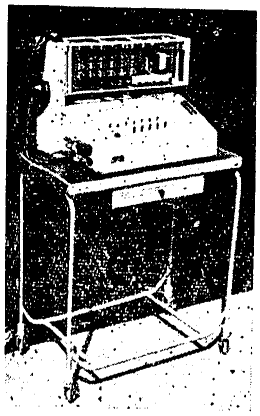

4

There are 20 removable rotating mounting plates installed in any combination on both sides of the RSL-DSh-ATS rack. The receivers are included in the plate assemblies and the generators in the rack, but they may be ordered separately as operational spares.

Angle brackets installed in the rack's top and bottom faces are included in the equipment kit for mounting the rack in standard metal-frame two-motion selector automatic telephone exchanges. The rack dimensions with the angle brackets are 2600x550x378 mm. The center-to-center installation distances are 2330 mm for the height, 400 mm for the width.

As was pointed out earlier, the RSLI-D assemblies can be used both on physical lines and in transmission channel systems with a separated signal channel. In the latter case, the interaction signals are transmitted along the signal channel at a frequency of 3800-3850 Hz with a pulse-length code adopted for transmission by inductive methods.

The RSLUT-D sets are free from the shortcomings inherent in signal transmission by inductive methods. The interaction signals are transmitted along two signal channels, one of which is formed by the transmission system and the other of which is formed directly by the assembly at a frequency of 2600 Hz. The signal code is devised in such a way that the 2600 Hz signals are transmitted when voice signals are not being conducted along the channel. This reduces the possibility of spurious cycling of the receiver due to voice signal currents. The 2600 Hz frequency is transmitted at a level of -26 dB in order to protect the transmission system's group circuit from overloads.

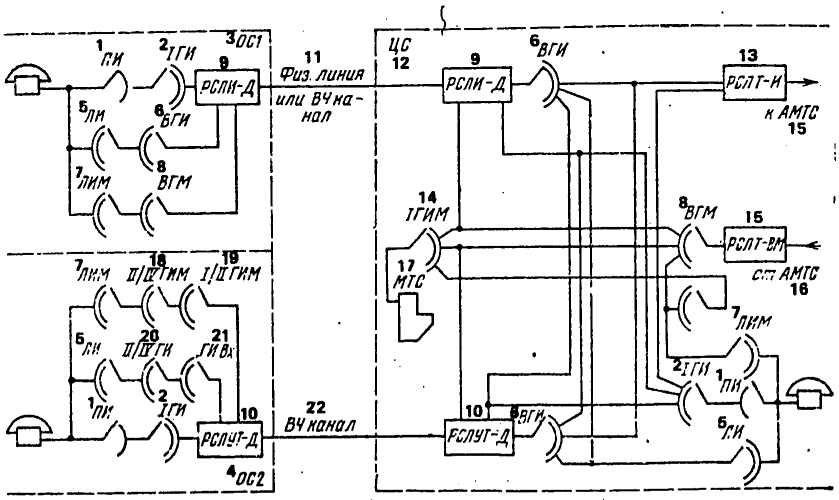

Fig. 5

1 - Preselector; 2 - First group selector; 3 - Terminal station No 1; 4 - Terminal station No 2; 5 - Final selector; 6 - Incoming selector; 7 - Trunk offering selector; 8 - VGM [expansion not provided]; 9 - RSLI-D; 10 - RSLUT-D; 11 - Physical line or HF channel; 12 - Central office; 13 - RSLT-I; 14 - First trunk group selector; 15 - RSLT-VM; 16 - From automated toll central office; 17 - Trunk exchange; 18 - Second and fourth trunk group selectors; 19 - First and second trunk group selectors; 20 - Second and fourth group selectors; 21 - Incoming selector; 22 - HF channel.

Таблица 1

1 Наименование оборудования	2 Габариты, мм	3 Масса, кг	4 Потребление тока, А, при напряжении 60 В
5 Статив РСЛ-ДШ-АТС (без плат)	2200×550×378	100	0,5
6 Плата РСЛИ-Д	516×160×140	11	0,45
7 Плата РСЛУТ-Д (с приемником)	516×160×140	9	0,2
8 Пульт ПП-РСЛ	384×507×350	18	0,5
9 Тележка	796×740×421	15	—
10 Генератор Г-2600-К	145×112×27	0,2	0,03
11 Приемник П-2600-2	145×112×27	0,2	0,03

Table 1

1 - Equipment designation; 2 - Dimensions, mm; 3 - Weight, kg; 4 - Current requirement, A, at 60 V; 5 - RSL-DSh-ATS rack (without mounting plates); 6 - Mounting plate RSLI-D; 7 - Mounting plate RSLUT-D (with receiver); 8 - PP-RSL control panel; 9 - Cart; 10 - G-2600-K generator; 11 - P-2600-2 receiver.

During two-way conversations on the signal channels, signalling frequencies are transmitted. This makes possible the uninterrupted monitoring of the channel's working order.

Central office or junction center of ATS-100/500, (100/500M), ATS-54 (54A) automatic exchange		Terminal or junction automatic exchange	
	Connecting line	Two-motion selector ATS-100/500 (100/500M)	Crossbar system ATSK-50/200M
RSLI-D	Physical line or HF channel	RSLI-D or RSL-100/500	RSLI-K
RSLUT-D	HF channel	RSLUT-D	RSL-VCh
RSL-100/500	Physical line or HF channel	RSLI-D	--

Table 2

Table 3

1 Характеристика	2 РСЛИ-Д	3 РСЛУТ-Д
4 Длительность управляющего сигнала, мс:		
5 индуктивный длинный	70—110	—
6 индуктивный короткий	20—30	—
7 набор номера	40—50	40—50
8 разъединение при работе по ВЧ каналу	250—350	—
9 Время распознавания длинного импульса, мс	40—55	—
10 Время распознавания короткого сигнала, мс	7—15	—
11 Время распознавания сигнала разъединения, мс	120—220	—
12 Искажения приемного реле, мс	±4	—
13 Амплитуда индуктивных импульсов, В, не менее	80	
14 Время срабатывания сигнального реле, мс:		
15 СА через устройство ЭУ-43, не более	70	70
16 СБ через устройство ЭУ-25	—	200—500
17 Задержка выдачи частоты f_1 при передаче сигнала занятия, мс	—	40—50
18 Задержка между сигналом f_2 и выдачей f_1, мс, не менее	—	20
19 Рабочее затухание, дБ, не более:	0,5	—
20 на передаче	—	12,5—13,5
21 на приеме	—	10,5—11,5
22 в режиме двухпроводного транзита:		
23 на передаче	—	5,3—6,7
24 на приеме	—	3,3—4,7
25 Переходное затухание, дБ, не менее:		
26 между разговорными цепями комплектов	78	78
27 с тракта приема на тракт передачи	—	50
28 Затухание асимметрии разговорных проводов относительно земли, дБ, не менее	43	43
29 Время разделения разговорного тракта, мс	—	50—75
30 Средняя наработка на отказ, цикл	20000	20000

1 - Characteristic; 2 - RSLI-D; 3 - RSLUT-D; 4 - Duration of pilot signal, ms; 5 - Long inductive; 6 - Short inductive; 7 - Number selection; 8 - Disconnection when operating on HF channel; 9 - Time of recognition of long impulse, ms; 10 - Time of recognition of short signal, ms; 11 - Time of recognition of disconnection signal, ms; 12 - Receiver relay deflection, ms; 13 - Amplitude of inductive pulses, V, not less than; 14 - Time of relay operation, ms; 15 - CA signal through EU-43 unit, not more than; 16 - CB signal through EU-25 unit; 17 - Delay in output of f_1 frequency when busy signal is transmitted; 18 - Delay between relieving of f_2 and output of f_1, ms, not less than; 19 - Operational attenuation, dB, not more than; 20 - Upon transmission; 21 - Upon reception; 22 - During two-line tandem operations; 23 - Upon transmission; 24 - Upon reception; 25 - Crosstalk attenuation, dB, not less than; 26 - Between voice circuits in the units; 27 - Between receiving and transmitting lines; 28 - Attenuation of asymmetry of voice lines relative to the ground, dB, not less than; 29 - Time separation of voice circuit, ms; 30 - Average number of cycles without malfunction.

A diagram for the organization of communications when the RSL-DSh-ATS equipment is used is shown in fig. 5. The RSLT-I and RSLT-VM assemblies shown in the diagram belong to the zonal automatic telephone communications equipment.

In table 2 are given possible operational combinations of the trunk relay assemblies when they are used at terminal (tandem) two-motion selector or crossbar automatic exchanges.

The establishment of the local call takes place when the terminal station subscriber selects an outgoing number for a tandem exchange or central office, and a physical line or HF transmission system channel through a free unit of the trunk relay becomes engaged. A trunk relay set and the equipment for the incoming automatic exchange become engaged at the central office (or tandem exchange). Provisions have been made in the RSLUT-D assembly for releasing the channel 10 to 20 minutes after the called subscriber hangs up if the caller continues to maintain the connection.

In order to establish an outgoing trunk connection after reaching the central office, the subscriber dials an outgoing number for a zonal automatic trunk exchange and engages a free RSLT-I unit. An outgoing call to the automatic trunk exchange is possible only in those cases when the terminal station (tandem exchange) is equipped with AON [automatic number identification] equipment. The transmission of "AON interrogation" and "Removal of AON interrogation" signals is insured by the RSL-DSh-ATS equipment.

The establishment of the incoming trunk connection takes place under the control of the automatic trunk exchange's instruments.

The electrical characteristics of the RSL-DSh-ATS equipment are cited in table 3.

The operation of the equipment as well as the routine maintenance and repair of the assemblies should be carried out using the PP-RSL control panel. The panel is equipped with a voice ringing set and technical instructions.

BIBLIOGRAPHY

1. Melamud, E. A. "New Techniques for the Transmission of Interaction Signals Between Rural Automatic Telephone Exchanges," VESTNIK SVYAZI No 5, 1975.

[222-9512]

9512
CSO: 1860

UDC 621.373.42

ANALYSIS OF THE EFFECT OF IONIZING RADIATION ON SELF-EXCITED OSCILLATOR FREQUENCY STABILITY

Moscow RADIOTEKHNIKA in Russian Vol 35, No 3, 1980 pp 42-44

[Article by V. P. D'yachkin and S. N. Krasil'nikov]

[Text] As a result of the effect of ionizing radiation on electronic devices (ED), the parameters of input signals from circuits of practically all types change [1,2], including transistorized, self-excited oscillators. Let us examine the stability of a self-excited generator frequency when exposed to ionizing radiation.

It is known that the equation for the stationary mode of a self-excited oscillator may be written in the form

$$\dot{Z}\dot{S}_{ave}K_{o.c}=1, \qquad (1)$$

where $\dot{Z}$ is the impedance in the collector circuit; $\dot{S}_{ave}$ is the average transconductance of the active element and K_{os} is the feedback factor.

Let us write the phase balance in the self-excited oscillator under the condition of dependence of the parameters of its elements α_1, α_2, ... α_n on an integral ionizing radiation flow ϕ:

$$\varphi=P[\alpha(\Phi), A, \omega]=\mp 2\pi m,$$

where A, ω are the amplitude and the frequency of the oscillations being generated.

To insure a stationary mode when there is radiation, the values of the amplitude and frequency of the oscillations being generated should vary so as to compensate for the increase in the elements' parameters.

Having expanded function P into a Taylor series by small increments of $\Delta\phi$, ΔA, $\Delta\omega$ around the point of stationary mode "0" and having been restricted by the linear members of the expansion, we obtain

$$\sum_{n=1}^{l}\left(\frac{\partial\varphi}{\partial\alpha_n}\right)\left(\frac{\partial\alpha_n}{\partial\Phi}\right)\Delta\Phi+\left(\frac{\partial\varphi}{\partial A}\right)\Delta A+\left(\frac{\partial\varphi}{\partial\omega}\right)\Delta\omega=0. \qquad (2)$$

Then the radiation change in the frequency of a self-excited oscillator will be

$$\frac{\Delta\omega}{\omega} \approx -\frac{\sum_{n=1}^{l}\left(\frac{\partial\varphi}{\partial\alpha_n}\right)\left(\frac{\partial\alpha_n}{\partial\Phi}\right)\Delta\Phi+\left(\frac{\partial\varphi}{\partial A}\right)\Delta A}{\left(\frac{\partial\varphi}{\partial\omega}\right)_{\omega}}. \qquad (3)$$

Let us compare the phase balance equation for the equivalent circuit for the self-excited Hartley oscillator in Figure 1 (where R_{out} and X_{out} are the output resistance and capacitive reactants of the transistor and $X_{ext} = (\omega C_{ext})^{-1}$ is the external reactance). Let us assume that $\dot{Z}_1$ and $\dot{Z}_2$ are purely reactive in nature; then $\dot{Z}_1 = iX_1 = i\omega L$; $\dot{Z}_2 = iX_2 = (i\omega C_2)^{-1}$ (the case of a capacitor-type Hartley oscillator.)*

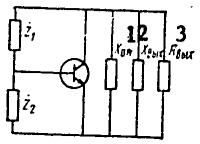

Puc. 1

Figure 1

Key to Figure 1:

1. X_{ext}
2. X_{out}
3. R_{out}

For convenience in analyzing the circuit we will convert the parallel connection R_{out}, X_{out} and X_{ext} into a series circuit R_3, X_3:

$$\dot{Z}_3 = \frac{R_{out}}{1+\omega^2C^2R_{out}} - i\frac{\omega CR_{out}^2}{1+\omega^2C^2R_{out}},$$

where $C = C_{ext} + C_{out}$; C_{out} is the output capacitance of the transistor. For the circuit being examined, it is here possible to write

$$\dot{Z} = \frac{(\dot{Z}_1+\dot{Z}_3)\dot{Z}_2}{\dot{Z}_1+\dot{Z}_3+\dot{Z}_2}; \qquad (4)$$

We will represent the feedback factor without taking into consideration the transistor input curve for simplification of further computation (i.e., we will suppose that K_{OS} is equal to the transformation coefficient):

$$\dot{K}_{o.s} = -\frac{\dot{Z}_3}{\dot{Z}_1+\dot{Z}_3}. \qquad (5)$$

*Rus. 'yemkostnaya trekhtochka,' possibly a Colpitts oscillator.

The average transconductance of the transistor [3] is

$$\dot{S}_{ave} = S_{ave}(1 + i\,tg\,\varphi_S)\cos\varphi_S, \qquad (6)$$

where S_{ave} and φ_s are the modulus and the phase of the average transconductance of the active element.

Having substituted (4) - (6) in (1), we obtain

$$-S_{ave}(1 + i\,tg\,\varphi_S)\cos\varphi_S \frac{\dot{Z}_1\dot{Z}_3}{\dot{Z}_1 + \dot{Z}_2 + \dot{Z}_3} = 1. \qquad (7)$$

The imaginary part of expression (7), taking into consideration the values Z_1, Z_2, Z_3 reflects the phase balance in the self-excited oscillator.

$$\omega C_1 R_{out} - tg\,\varphi_S \omega^2 C R_{out} C_1 + i D_1 = 0, \qquad (8)$$

where

$$D_1 = 1 + \omega^2 C_1 (CR_{out}^2 + L) + \omega^4 R_{out}^2 C^2 (1 + \omega L C_1);\ t = tg\,\varphi_S + \omega C R_{out}$$

As is known [4], the main causes of frequency instabilities in transistorized, self-excited oscillators are changes in the output capacitance, in the transistor transconductance phase. If a self-excited oscillator is examined at frequencies $0.1\ \omega_S \leq \omega \leq 0.3\ \omega_S$ (where ω_S is the limiting transconductance frequency of the transistor), when frequency instability because of changes in transconductance phase may be ignored [5]. Furthermore, the average transconductance phase within the frequency range under examination does not depend on amplitude [6], therefore we take the second member in the numerator of formula (3) to be equal to zero.

The stability of the passive elements of circuits to the effect of ionizing radiation is much higher than in transistors [7], therefore the radiation change in their parameters cannot significantly affect the frequency being generated. The output capacitance of a transistor in a circuit with an OE [common emitter] is usually written as

$$C_{out} \approx C_{bc}(1 + h_{21e}), \qquad (9)$$

where C_{bc} is the barrier capacitance of the collector p-n-junction; h_{21e} is the coefficient of base current transmission.

The absolute radiation change h_{21e} is much greater than the change of C_{bc}, therefore we exclude the latter from analysis. Given a radiation by an integral flow, $\phi \geq \phi_a$ (ϕ_a is the integral absolute transistor stability flow) and h_{21e} varies according to the rule [1]

$$h_{21e\phi}^{-1} = h_{21e}^{-1} + \frac{0{,}2\Phi}{K_\phi f_\tau}, \qquad (10)$$

where K_f is the coefficient of radiation damage depending on the resistivity of the material in the transistor base and the ionizing radiation energy; f_T is the limiting frequency of the transistor transmission coeffieient; h_{21ef} is the transistor base current transmission coefficient after irradiation.

Having substituted formulae (8) - (10) in (3), and after appropriate transforms, we obtain

$$\left.\begin{aligned}\frac{\Delta\omega}{\omega} = \frac{VR_{вых}\omega(\operatorname{tg}\varphi_S R_{вых}\omega C_1 - D_1) - tVR_{вых}^2\omega^2(C_1 + 2C + 2L\omega^2 C C_1)}{R_{вых}C_2 - 2\operatorname{tg}\varphi_S R_{вых}\omega C_1\tau + D_1\tau + 2\omega t(R_{вых}C_1\tau + \tau^2 + LC_1 + 2L\omega^2 C_1\tau^2)} \times \\ \times \frac{0{,}2\Delta\Phi}{K_\Phi f_\tau}; \\ \tau = R_{вых}C;\ V = C_{к.б}h_{21э.0}^2.\end{aligned}\right\} \quad (11)$$

In a circuit with inductive feedback:

$$\dot{Z}_1 = iX_1 = (i\omega C_1)^{-1};\ \dot{Z}_2 = iX_2 = i\omega L_2;\ \dot{Z}_3 = R_3 + iX_3;\ X_{вн} = \omega L.$$

the values of R_3 and X_3 take on the form

$$R_3 = \frac{\omega^2 L^2 R_{out}}{(R_{out} - \omega^2 C_{вых} L R_{out})^2 + (\omega L)^2};\ X_3 = \frac{\omega L R_{out}(R_{out} - \omega^2 C_{вых} L R_{out})}{(R_{out} - \omega^2 C_{out} L R_{out})^2 + (\omega L)^2};$$

since it is usually true that $\omega L >> (R_{out} - \omega^2 C_{out} L R_{out})$, the first term in the demoninators may be ignored. In this case, $R_3 \approx R_{out}$; $X_3 \approx M/\omega L$ [here $M = R_{out}^2 (1 - \omega^2 C_{out} L)$].

Performing all subsequent calculations, as we did for self-excited oscillators with a capacitive feedback, we find

$$\frac{\Delta\omega}{\omega} = \frac{\omega^2 L R_{out} V(D_1 + \omega C_1 M)}{(\operatorname{tg}\varphi_S - 2\omega C_{out} R_{out}) L R_{out} D_1 + (\operatorname{tg}\varphi_S R_{out}\omega L + M)\frac{\partial D_1}{\partial\omega} + \eta} \frac{0{,}2\Delta\Phi}{K_\Phi f_\tau}, \quad (12)$$

where

$$D_1 = M\omega C_1 + \omega^3 L L_1 C_1 + \omega L_1;\ \eta = \omega L C_1 R_{out}(2\omega^2 L R_{out}^2 C_{out}\operatorname{tg}\varphi_S - 3\omega L R_{out} - 2\operatorname{tg}\varphi_S M)$$

Experimental tests were made to check the ratios which were obtained. Self-excited oscillator units were irradiated using neutrons with an energy of 0.1 MeV in the horizontal experimental channel of a nuclear reactor. The thermal neutron component of the complex field of the reactor's active zone was weakened using a cadmium shield. Preliminary control of the exposure value for the integral neutron flow was provided based on a radiation time and the reactor's power. The final value of the integral flow acting on the self-excited oscillators was determined from calibrated threshold detectors which were irradiated along with the samples.

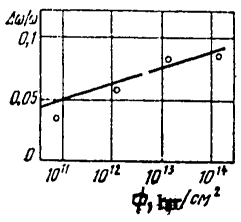

Рис. 2

Figure 2

As may be seen from Figure 2, the calculated data from formula (11) coincide with the results of full-scale testing with an accuracy adequate for practice. In making the calculations, an integral neutron equal to ϕ_a was taken as the small increase in the integral flow $\Delta\phi$. The relationships (11) and (12) permit us to calculate the radiation-parametric frequency drift in LC-self-excited oscillators with an inductive and a capacitive feedback and may prove to be useful in engineering practice.

LITERATURE

1. Vavilov, V. S.; Ukhin, N. A. "Radiatsionnyye effekty v poluprovodnikakh i poluprovodnikovykh priborakh [Radiation Effects in Semiconductors and Semiconductor Devices]," Moscow, Atomizdat, 1969.

2. Korshunov, F. P.; Gatal'skiy, G. V.; Ivanov, G. M. "Radiatsionnyye effekty v poluprovodnikovykh priborakh [Radiation Effects in Semiconductor Devices]," Minsk, Nauka i teknika, 1978.

3. Al'tshuller, G. B. "Kvartzevaya stabilizatsiya chastoty [Quartz Frequency Stabilization]," Moscow, Svyaz', 1974.

4. Chelnokov, O. A. "Poluprovodnikovyye pribory i ikh primeneniye [Semiconductor Devices and their Application]," Moscow, Sov. radio, No. 6, 1960.

5. Al'tshuller, G. B.; Murzin, V. I.; Panfenov, B. G. "Poluprovodnikovyye pribory v teknike elektrosvyazi [Semiconductor Devices in Electrocommunications Engineering]," Moscow, Svyaz', No. 6, 1970.

6. Savel'yev, S. A.; Chelnokov, O. A. "Poluprovidnikovyye pribory i ikh primeneniye [Semiconductor Devices and their Application]," Moscow, Sov. radio, No. 18, 1967.

7. Goryachev, G. A.; Shapkin, A. A.; Shirshev, L. G. "Deystviye pronikayushchey radiatsii na radiodetali [The Effect of Penetrating Radiation on Radio Components]," Moscow, Atomizdat, 1971.

8. Stepanenko, I. P. "Osnovy teorii tranzistorov i tranzistornykh skhem [Fundamentals of Transistor and Transistor Circuit Theory]," Moscow, Energiya, 1977.

9194
CSO: 1860

PUBLICATIONS, INCLUDING COLLECTIONS OF ABSTRACTS

PAPERS ON ELECTRONIC TECHNOLOGY

Kiev, VESTNIK KIYEVSKOGO POLITEKNICHESKOGO INSTITUTA; RADIOELECTRONIKA (Bulletin of the Kiev Polytechnical Institute; Radioelectronics) in Russian, No 16, 1979 signed to press 4 Jan 79 p 2, 132-135

[Annotation and table of contents from journal edited by A. Ye. Balyasnaya, Vishcha shkola, 1000 copies, 144 pp]

[Text] This bulletin deals with issues in the analysis and synthesis of electronic circuits, the development of methods and devices for transforming information, the study of the electrophysical characteristics of solids and their use in the development of electronic technology.

For scientific workers and engineers in appropriate specialities.

CONTENTS

Altayskiy, Yu.M., Sytenko, T. N., Lositskaya-Yezhova, L. G. Measurement of the initial bend zone in β-SiC models using a strong signal photo e.m.f..... 3

Tyagul'skiy, I. P., Lositskaya-Yezhova, L. G. The influence of diffusion length of minority carriers on photoelectric memory in epitaxic n-GaAs..... 4

Sidyakin, V. G., Podlasov, S. A., Gayevskiy, O. K. Thermo e.m.f. in SiC 6H crystals..... 6

Kravchuk, A. F. An algorithm for computing generalized Fermi-Dirac intervals..... 9

Korobanov, V. L., Novominskiy, B. A., Novominskiy, V. A. Effective Hall mobility in layers of enrichment of electronic germanium.....

Kolyada, Yu. V., Vityaz', O. A. On the selection of an initial approximation in the solution of systems of nonlinear equations of a special type..... 18

Il'chenko, A. N. Modelling circuits with ideal multiband components in a uniform coordinate base..... 20

Il'chenko, A. N. The calculation of transistor circuits in constant current mode..... 24

Pigilov, I. A., Shelkovnikov, B. N. Computer algorithms of harmonic analysis of nonlinear electronic circuits based on a rapid Fourier transform on the basis of Vilenkin-Krestenson functions..... 26

Shalayev, V. A., Genis, Ye. A., Spirin, A. Yu. Models and algorithms for computer projection of directional couplers on coupled lines... 28

Zhabitskiy, V. P., Prikhod'ko, A. A. A computer implemented statistical analysis of electronic circuits in differential operational amplifiers..... 30

Krizhanovskiy, V. I., Shendakov, A. I. On the cathode drop in potential of glow discharge in a transverse magnetic field..... 33

Mel'nik, V. I., Novikov, A. A. The derivation of the basic parameters of gas discharge electron sources with anode plasma..... 38

Shmyreva, L. N. Toward the calculation of erosion of electrodes in a high current discharge arc in powerful discharges..... 41

Sheyko, Yu. A. An equivalence diagram and the coefficient of electromechanical bonds in a flexing oscillating piezoelectric resonator..... 46

Klochko, S. F. Broad band selective piezoelectric filters..... 49

Vakulenko, Ye. M., Tsurin, O. F. The obtaining of operative control of the rotation of complex images..... 52

Machugovskiy, V. S. A general description of the input language for describing the object of study of a system of programs for the analysis of radioelectronic circuits..... 54

Timchenko, A. P., Ladogubets, V. V., Vlasov, A. I. A program for obtaining symbolic operator expressions for transmission functions. 56

Tsurin, O. F., Zaichenko, L. Ye., Salova, Ye. V. Issues in the design of dialogue systems..... 58

Kuz'michev, A. I. De-ionization in the presence of a current through a plasma..... 59

Zashivaylo, T. V. Materials for input openings of pyroelectric tubes..... 64

Pogorelova, G. F., Chadyuk, V. A. The measurement of midget linear and angular displacement using lasers..... 69

Ayvazova, A. S., Shvarts, I. M. On the influence of alloying ... several electrical characteristics of β-SiC monocrystals..... 73

Trifonyuk, V. V., Sen'ko, V. I., Morozov, V. G. A diode-transistor generator of sawtooth voltage..... 75

Druzhinin, N. V., Starikov, V. A., Tyupa, A. N. The "electronic magnifying glass" in a storage block in CRT storage..... 78

Pankov, S. N., Petinov, V. P., Shalayev, V. A. Algorithms for models of SVCh (microwave) elements..... 80

Serbin, S. A. Some issues in the analysis of methods of editing the results of computer generated representations in a visual-graphic form..... 82

Ruban, A. S., Popuch, V. S., Artyukhov, V. G. A digital real-time filter..... 86

Kokoshkin, S. M. Study of the metrological characteristics of a time-scale transformer of time-intervals..... 90

Kosinov, N. V., Abakumov, V. G., Leskin, V. F. An analysis of multi-station systems by queuing theory methods..... 93

Petrenko, A. I., Drizhchanyy, S. A., Leskin, V. F. The construction of indicators for representing information in a three dimensional form..... 96

Druzhinin, N. V. On automatic change of mode in CRT storage..... 98

Lysenko, A. Ye. On the evaluation of the technical level of video terminal devices..... 101

Belousov, V. D., Shkuro, A. N. Potential capabilities of a method of transforming time scale by means of CRT storage with a broad band modulator..... 103

Terletskiy, A. V. A device for transforming of Roentgen television images on storage CRT..... 105

Terletskiy, A. V., Shpakovskiy, A. A. Mode comutators for CRT storage..... 108

Mel'nik, A. S. The organization of a library of transistor models for a system of automated ...esign..... 112

Sytenko, T. N., Zimenko, V. I., Tyagul'skiy, I. P. Equipment for investigating level parameters on the interface between dielectric-semiconductor structures by a thermally inducing charge release in a temperature range of 4.2-300 K..... 114

Khreshchenyuk, A. P., Kusaylo, V. P. A digital analogue device for the transformation of coordinate axes..... 117

Balanovskaya, O. Yu., Vasil'yeva, L. D. On increasing the sensitivity of pyroelectric targets..... 120

Sinekop, Yu. S., Chekhlov, A. N. An experimental study of structural interference in oscillographic stroage CRTs..... 122

Levchenko, G. T., Prez, A. A. A film electroacoustical radiator..... 123

Kuz'michev, A. I. Modeling the control of breakdown in plasma cathode apparatus..... 125

Denbnovetskiy, S. V., Antonets, V. P., Kreydich, Ye. A., Lyakhovetskiy, A. I., Orlov, I. I. Television apparatus in a system of devices for technical instruction..... 129

9285
CSO: 1860

RADARS, RADIO NAVIGATION AIDS, DIRECTION FINDING, GYROS

UDC 621.393.96

EXPANDING THE LIMITS OF THE APPLICABILITY OF A MATHEMATICAL RADAR TARGET MODEL

Moscow RADIOTEKHNIKA in Russian Vol 35, No 3, 1980 pp 44-46

[Article by Ye. D. Kazakov]

[Text] The mathematical models being used to produce an expression for the reflected signal of radar targets in the quasi-optical area of radio wave dispersion [1,2] are valid when all of the distances l_i between the target reflection elements[1] are considerably greater (by an order) than the maximum wavelength of the radar station λ.

In practice, actual radar targets may have a large number of reflecting elements. This results in a reduction of the distances between the individual reflectors, and the use of mathematical target models for analyzing information contained in the reflected signal, in particular the model described in [1] will result in significant errors. Below for a more general model, which makes it possible to take into account the polarization-frequency properties of the reflected signal [2], additional conditions are introduced which permit us to expand the limits of applicability of the model, i.e., load to the possibility of using the model in the case when certain distances between the target reflecting elements become commensurate with the wavelength of the radar station. Let us obtain and analyze the expression for the average value for the matrix of the intensities of signals reflected from the target for introduction of these conditions.

Let the radar station radiate a signal on two orthagonally polarized frequencies and reception of the reflected signal be accomplished by two orthagonally polarized receiving channels. Then the matrix of the reflected signals when representing a target consisting of N independent reflecting elements [2] may be written in the form

[1]Any kind of reflectors on the target, the reflecting properties of each of which are characterized by their polarization dispersion matrix in the polarization base of a radiating radar station [2], are called the target reflecting elements.

where $m = 2\pi/\lambda$ is the wave number; $x_i(t)$ is the coordinate of the i-th target reflecting element, read off from the reference center of the target along the sighting line; $r(t)$ is the distance to the reference center of the target; $S_i(t)$ is the polarization dispersion matrix (pdm) of the i-th target reflecting element in the polarization measuring base of the radar stations; $U(t-t_0)$ is the matrix of the radar station's radiated signals delayed for the propagation time t_0 up to the target reference center.

The expression for the average value of intensity of the reflected signal of the main constituent upon averaging over a certain time interval[2], which is analogous to averaging the observation angles at a certain angle of approach, has the form

$$\overline{E_{pp}^2(t)} = \sum_{i=1}^{N} \overline{S_{ppi}^2(t) U_p^2(t-t_0)} + \sum_{i\neq l,\ l=1,\ i=1}^{N} \overline{\dot{S}_{ppi}(t)\dot{S}_{ppl}^{*}(t) U_p^2(t-t_0) e^{j2m[x_i(t)-x_l(t)]}}. \qquad (2)$$

where $\overline{}$ is the sign for time-dependent averaging.

Since the target orientation and nature of its rotation are unknown, we assume that change in the observation angle of the radar target is a random, stationary ergodic process. Then when calculating the average value of the intensity of the reflected signal, it is possible to switch from time-dependent averaging to statistical averaging. In this case each member of the second sum of expression (2) is divided into two cofactors because the values of S determine the reflecting properties of the individual reflectors and the exponential cofactors are the position of the reflectors in space. The average value for the intensity of the reflected signal is in this case expressed in the values of the effective target reflecting surface.

$$\langle S_{pp}^2(t)\rangle = \sum_{i=1}^{N} \langle S_{ppi}^2(t)\rangle + \sum_{i\neq l,\ i=1,\ l=1}^{N} \langle \dot{S}_{ppi}(t)\dot{S}_{ppl}^{*}(t)\rangle \langle e^{j2m[x_i(t)-x_l(t)]}\rangle. \qquad (3)$$

Expression (3) is distinct from those expressions usually cited in the literature, e.g., in [1] because of the presence of the second sum. Since the first member of (3) is the sum of the average values of the

[2]The averaging interval is determined by the relationship of the target dimensions and the wave length of the radar station.

effective reflecting surfaces of the target's reflectors on fundamental polarization, consequently it is necessary to reduce the second sum to zero in order to obtain the well-known expression from (3).

Let us obtain the dependence of the exponential property of expression (3) on the target deflection angle in explicit form. Let target rotation occur in the plane XOY (cf figure) and let the rotation speed of all the target reflecting elements be identical ($\Omega_i = \Omega_i = \Omega$). Then if the sector of the observation angles is small and rotation begins at the instant characterizable by the angle's $\mathcal{E}_{10}$, $\mathcal{E}_{10}$, then

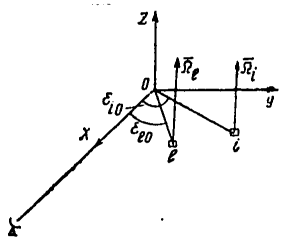

Puc. 1

Figure 1

$$x_i(t) - x_i(t) = \rho_{i0}\cos(\varepsilon_{i0} + \Omega t) - \rho_{e0}\cos(\varepsilon_{e0} + \Omega t).$$

Transforming this expression we obtain $x_i(t) - x_i(t) = \Delta x_{i1e}\cos\Omega t + \Delta y_{i1e}\sin\Omega t$, where Δx_{1i_0}, Δy_{1i_0} are the distance between the 1-th and i-th target reflectors at the initial instant along axes x and y of the coordinate system.

For a small observation angle sector, this expression may be written in the form

$$x_i(t) - x_i(t) = \Delta x_{i1_0}\sqrt{1-\gamma^2} + \Delta y_{i1_0}\gamma, \qquad (4)$$

where $\gamma = \Omega t$.

Substituting (4) in (3), we obtain

$$\langle S^2_{pp}(t)\rangle = \sum_{i=1}^{N}\langle S^2_{ppi}(t)\rangle + \sum_{\substack{i=1,\ i=1\\ i\neq l}}^{N}\langle \dot{S}_{ppi}(t)\,\dot{S}^{*}_{ppl}(t)\rangle\left\langle e^{i\frac{4\pi}{\lambda}\left(\Delta x_{i1_0}\sqrt{1-\gamma^2}+\Delta y_{i1_0}\gamma\right)}\right\rangle. \qquad (5)$$

When the differences in the coordinates at the initial instant are independent and when there are normal laws for the distribution of the coordinates of the reflecting elements along axes x and y with zero average values and standard variation of σ_{xio}, σ_{xlo}, σ_{yio}, σ_{ylo} we have [3],

$$J = \exp\left\{-\frac{8\pi^2(1-\gamma^2)}{\lambda^2}\left(\sigma^2_{x_{i0}} - 2r_{x_{i0}x_{l0}}\sigma_{x_{i0}}\sigma_{x_{l0}} + \sigma^2_{x_{l0}}\right)\right\}\times$$
$$\times\exp\left\{-\frac{8\pi^2\gamma^2}{\lambda^2}\left(\sigma_{y_{i0}} - 2r_{y_{i0}y_{l0}}\sigma_{y_{i0}}\sigma_{y_{l0}} + \sigma^2_{y_{l0}}\right)\right\}. \qquad (6)$$

Let us examine the physical sense of the coefficients of correlation among the reflector coordinates $r_{x_{io}x_{lo}}(r_{y_{io}y_{lo}})$.

Expression (6) approaches zero if the exponential properties increase. In this case (3) is reduced to the known expression, i.e., the mathematical model based upon which the expression for the reflected signal was obtained, will be valid. Let

$$r_{x_{i0}x_{l0}}(r_{y_{i0}y_{l0}}) = 1, \quad \left|(\sigma_{x_{i0}} - \sigma_{x_{l0}})/\lambda\right| \gg 1, \left|(\sigma_{y_{i0}} - \sigma_{y_{l0}})/\lambda\right| \gg 1$$

(the distance among the coordinates of pairs of target reflecting elements is significantly greater than the radar station's wave length.)

Then, (6) approaches zero and (3) transforms into

$$\langle S^2_{pp}(t)\rangle = \sum_{i=1}^{N} \langle S^2_{ppi}(t)\rangle. \qquad (7)$$

When the coefficient of correlation between the coordinates for the pairs of target reflecting elements is equal to unity, it is necessary that the distances between the reflector coordinates significantly exceed the radar station's wavelength for applicability of the radar target model being used.

In order to reduce the second sum in (3) to zero when the distances between the reflectors are diminished, but still exceed the radar station's wavelength, the value for the coefficient of correlation between the coordinates of the reflector pairs in (6) should vary from one to minus one.

This additional condition will permit us to expand the limits of applicability for the proposed mathematical model. It is advisable to introduce analogous values for the coefficients of correlation into multiples between the coordinates of the depolarizing target reflecting elements when obtaining and using expressions of the reflected signal for depolarized constituents. Specific values for the coefficient of correlation between the coordinates of the target reflecting elements are selected for each pair of reflectors on the basis of the physical observation conditions for one or another of the targets when conducting concrete studies.

Thus introduction of coefficients of correlation between the coordinates of pairs both of all, as well as of just the depolarizing reflecting elements, the values of which diminished from one to minus one as the distance between the reflectors is reduced (as this distance approaches the radar station's wavelength), into the mathematical model of radar targets also permits us to use the mathematical model for the analysis of polarization-dispersing properties of tragets which is described in [2] in this case as well.

LITERATURE

1. "Teoreticheskiye osnovy radiolokatsii [Theoretical Fundamentals of Radar]," Ya. D. Shirman, ed. Moscow, Sov. radio, 1970.

2. Kazakov, Ye. L. RADIOTEKHNIKA, vol. 31, No. 4, 1976.

3. Levin, B. R. "Teoreticheskiya osnovy statisticheskoy radiotekhniki [Theoretical Fundamentals of Statistical Radio Engineering]," Pt. 1, Moscow, Sov. radio, 1969.

[217-9194]

9194
CSO: 1860

UDC 621.396.96

MULTICHANNEL SHORT-RANGE NOISE RADAR STATIONS WITH INTEGRAL SCAN

Moscow RADIOTEKHNIKA in Russian Vol 35, No 3, 1980 pp 35-37

[Article by V. V. Grigorin-Ryabov, A. P. Bogachev and O. I. Shelukhin]

[Text] In a number of instances, the task of detecting still objects with great accuracy over a strictly fixed territory in case of intense interfering reflections from an underlying surface and local objects is of interest. A similar problem is solved using stationary, short-range noise radar stations with integral scan [1]. Moreover, the high requirements imposed on the accuracy for determining the position of obstacles, and the noise immunity of the systems, as well as on fixation of the boundaries of the area being monitored make it necessary to build multichannel radar stations with space-time signal processing.

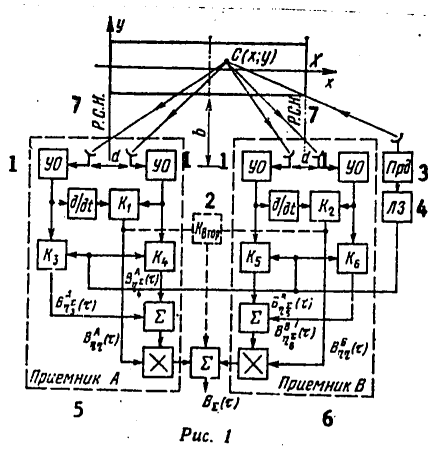

Рис. 1

Figure 1

[Key on following page]

Key to Figure 1:

1. Accelerator-limiter
2. K_{sec}
3. Prd [? Transmitter]
4. Delay line
5. Receiver A
6. Receiver B
7. Equisignal direction

Let us examine the main design features and the characteristics of similar systems, one configuration of which is shown in Figure 1. Two azimuth dual channel systems, the equisignal directions of which are coincident with the boundaries of the area being monitored, are used in the radar station receiver. Considering that the main signal represents a normal stationary random process with a prescribed energy spectrum

$$S_\xi(\omega) = \sigma_\xi^2 \frac{2\sqrt{\pi}}{\Delta\omega_c} \exp\left[-\frac{(\omega-\omega_c)^2}{\Delta\omega_c^2}\right], \quad \Delta\omega_c \ll \omega_c,$$

Let us determine the output characteristic of the dual channel system of, for example, receiver A:

$$B^A_{\eta'\eta}(\tau) = \frac{F(\psi_1)F(\psi_2)}{\pi}\int_0^\infty S_\xi(\omega)K_1(\omega)K_2(\omega)K_d(\omega)\,e^{j[\omega\tau+\varphi_1(\omega)+\varphi_2(\omega)-\varphi_d(\omega)]}d\omega, \quad (1)$$

where $K_1(\omega)$, $K_2(\omega)$ and $K_d(\omega)$ are the normed frequency characteristics of the first and second channels and the differentiator, respectively; $\phi_1(\omega)$, $\phi_2(\omega)$, and $\phi_d(\omega)$ are their phase characteristics, respectively; $F(\psi_1)$, and $F(\psi_2)$ are the radiation patterns of the receiving antennas; $\psi(x;y)$ is the angle between the normal to the antenna's aperture plane and the direction to the object.

We assume that the amplifier in each channel is a narrow-band linear system with a transmission band $\Delta\omega_i$ and amplitude-frequency characteristics similar to $S_\xi(\omega)$, e.g., in the form of a Gauss radio filter.

$$K_i(j\omega) = \exp\left[-\frac{1}{2}\left(\frac{\omega-\omega_{0i}}{\Delta\omega_i}\right)^2 - j\frac{2\pi(\omega-\omega_{0i})}{\Delta\omega_i}\right],$$

where $\Delta\omega_i$ is the transmission band at the level $1/\sqrt{e}$.

Substituting the values for $S_\xi(\omega)$ and $K_i(i\omega)$ in (1), and also assuming that $K_d(i\omega) = K_2(j\omega) = e^{-\frac{\pi}{2}}$, a $\omega_{01} = \omega_0 - \Delta\omega_{01}$ и $\omega_{02} = \omega_0 + \Delta\omega_{01}$,

we finally find

$$B_{\eta'\eta}[\tau(x;y)] = F[\psi_1(x;y)]F[\psi_2(x;y)]\frac{2\sqrt{\pi}\sigma_\xi^2}{\Delta\omega_c\sqrt{\chi_1}} \times$$

$$\times \exp\left[-\frac{(\sigma_1^2-\sigma_2^2)}{2} + \frac{1}{\chi_1}\left(\frac{\sigma_1}{\Delta\omega_1}-\frac{\sigma_2}{\Delta\omega_2}\right)^2\left(\tau(x;y) - \right.\right.$$

$$\left.\left. - \frac{1}{\sqrt{2}}\left(\frac{1}{\Delta\omega_1}+\frac{1}{\Delta\omega_2}\right)^2\right]\sin\left[\omega_c\tau(x;y) - \frac{\sigma_1+\sigma_2}{\sqrt{2}} - \frac{1}{2\chi_1}\times\right.\right.$$

$$\left.\left. \times\left(\frac{\sigma_1}{\Delta\omega_1}-\frac{\sigma_2}{\Delta\omega_2}\right)\left(\tau(x;y) - \frac{1}{\sqrt{2}}\left(\frac{1}{\Delta\omega_1}-\frac{1}{\Delta\omega_2}\right)\right)\right]\right]. \quad (2)$$

where

$$\alpha_l = \frac{\Delta\omega_{al}}{\Delta\omega_l}; \quad \chi_1 = \Delta\omega_0^{-2} + (2\Delta\omega_1^2)^{-1} + (2\Delta\omega_2^2)^{-1}.$$

As may be seen from (2), the presence of a rapidly changing function in $B_{\eta/\eta}[\tau(x;y)]$ may result in ambiguity in determining the angular coordinate of the object; however the direction properties of the radiation patterns permit us to eliminate the aforementioned ambiguity.

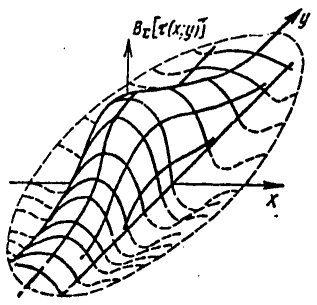

Puc. 2

Figure 2

Correlative processing of the noise signal in the units K_3, K_4, K_5 and K_6 calculating the function $B_{\eta,\xi}[\tau(x;y)]$ was specified to achieve higher range rasolution in the receiver. Moreover, the lag time of the reference signal is chosen from the relationship $\tau_{op} = 1/C(R_{01} + R_{02})$, a fact conditioned by the location of the transmitter and receiver's A and B in the foci of the ellipse, the generatrix of which passes through the geometric center of the territory being guarded. Range resolution in the systems being examined is primary determined by the broad band nature of the probing signal.

Let us determine the summary characteristic of a system having the structural diagram shown in Figure 1:

$$B_\Sigma[\tau(x;\ y)] = B^A_{\eta'/\eta}[\tau(x;\ y)]\left\{B^A_{\eta_1\xi}[\tau(x;\ y)] + B^A_{\eta_2\xi}[\tau(x;\ y)]\right\} + \\ + B^B_{\eta'/\eta}[\tau(x;\ y)]\left\{B^B_{\eta_1\xi}[\tau(x;\ y)] + B^B_{\eta_2\xi}[\tau(x;\ y)]\right\}.$$

A geometric interpretation of the summary characteristic of the system is presented in Figure 2. As we see, $B_\Sigma[\tau(x;y)]$ for objects located beyond the area being monitored and within its bounds is distinguished by polarity, which may be used to improve the angular coordinate resolution. This leads to partial compensation of interferring reflections from an underlying surface and local objects; for illustration let us determine the level of interferring reflections at the output of each of the azimuth systems, using the results of [2]

$$U_\Phi = L\int_{-\infty}^{\infty}\int F[\psi_{пер}(x;\ y)]\,F[\psi_1(x;\ y)]\,F[\psi_2(x;\ y)]\ B_{\eta'/\eta}[\tau(x;\ y)]\,V[\vartheta(x;\ y)]\,dx\,dy,$$

where $V[\vartheta(x;y)]$ is the specific effective reflecting area of the underlying surface; $\vartheta(x;y)$ is the angle of incidence of a wave at a point with coordinates x,y; L is a proportionality coefficient.

It is not difficult to demonstrate that given intensive interferring reflections from local objects, i.e., a clearly expressed background nonuniformity, the interferring reflections are partially compensated when there are identical receiving channels and a uniform underlying surface, i.e., when $V[\vartheta(x;y)] = \text{const.}$; when there are identical radiation patterns for the channels, full background compensation is observed. Let us examine several features of similar systems associated with a determination of their detection characteristics.

As was shown in [3], in the case of optimum processing of the channels it is possible to determine the detection characteristics using distribution cumulents which take on the following form for the case being examined:

$$\varkappa_1 = m\left[\det\|C\| + \frac{1}{2}\operatorname{tr}\|b\|\right]; \quad \varkappa_n = \frac{1}{n!}\, m \operatorname{tr}\|b^n\|; \quad n > 1,$$

where

$$C_{jk} = \ln\left[R_{jk(c.\,n)} R^{-1}_{jk(n)}\right]; \quad b_{jl} = \int_0^{T_l} R_{jk}(t;\tau)\, h_{kl}(\tau; S)\, d\tau;$$

m is the number of spatially separated receiving channels (in the given case, m = 4). For systems in Figure 1, the quadratric matrices C and B degenerate into block matrices of the form

$$C = \left\|\begin{array}{c|c} C_1 & 0 \\ \hline 0 & C_2 \end{array}\right\| \quad \text{и} \quad b = \left\|\begin{array}{c|c} b_1 & 0 \\ \hline 0 & b_1 \end{array}\right\|, \tag{3}$$

a fact caused by the spatial separation of the receiver channels or by $R_{13} = R_{14} = R_{23} = R_{34} = R_{31} = R_{41} = R_{32} = R_{43} = 0$.

As may be seen from (3), the spatial separation of the receiving channels as well as the need for forming and alternating characteristic $B_\Sigma[\tau(x;y)]$ results in the detection characteristics becoming worse. As engineering formulae permitting us to evaluate the detection characteristics we use the relationship $D = 1 - (1 - P_{t.d.\eta'\eta} P_{f.a.\eta\xi'})^4$ for the probability of correct detection D. By analogy, we use $F = 1 - (1 - P_{f.a.\eta'\eta} P_{f.a.\eta\xi})^4$ $4P_{f.a.\eta'\eta} P_{f.a.\eta\xi'}$ where P_{tdi} and P_{fai} are the probabilities of correct detection and false alarm for each of the processing channels.

To improve the probability of correct detection it is possible to use the secondary correlation phenomena for which correlative processing of signals from the outputs of the correlators K_1 and K_2 is performed (cf. Figure 1). Using this type of processing permits us to eliminate the block nature of matrices in (3) and it expands the potential capabilities of the system. Moreover, the probabilities of proper detection and false alarm may be determined from the relationship

$$D, F = 1-(1-P_{t.d}(\text{illegible}))(1-P_{t.d}(\text{illegible}))(1-P^2_{t.d}(\text{illegible})).$$

It is not difficult to see that in the latter instance, an increase in the probability of proper detection and a negligible increase in the probability of false alarm are observed.

Aside from the task of detecting obstacles within the bounds of the recorded area, the indicated systems may also evaluate the coordinates of the site of these obstacles. For this, for example, in the case of coincidence of the transmitter and receiver B, it is necessary to include in this system a device solving the system of equations

$$\left.\begin{aligned}\Delta\tau_1^* &= \frac{1}{C}\left(2R_0 - \sqrt{(0{,}5X+x)^2+(b+y)^2} - \sqrt{(0{,}5X-x)^2+(b+y)^2}\,C\right);\\ \Delta\tau_2^* &= \frac{2}{C}\left(2R_0 - \sqrt{(0{,}5X+x)^2+(b+y)^2}\right).\end{aligned}\right\} \quad (4)$$

From (4), after simple transforms, we find

$$\Delta\tau_1^* = \frac{2}{CR_0}(x^2+2by+y^2); \quad \Delta\tau_2^* = \frac{2}{CR_0}(x^2+Xx+2by+y^2),$$

where $\Delta\tau_1^*$ is an evaluation of the dealy of the signal reflected from the obstacle in receiver A, $\Delta\tau_2^*$ is the delay of the signal which is evaluated in receiver B.

It is not difficult to see that for receiver A, $\Delta\tau_1^*(x;y)$ = const is an ellipse, whereas for B, $\Delta\tau_2^*(x;y)$ = const is a circumference. Thus, the site of an object may be determined as the point of intersection of the ellipse and the circumference. The ambiguity of the solution of equations (4) may easily be eliminated by using the directional properties of the receiving antennas.

LITERATURE

1. Grigorin-Ryabov, V. V.; Shelukhin, V. I.; Shelukhin, O. I. Inventor's Cert. No. 510402 with priority since 18 January 1974.

2. Shelukhin, O. I. IZVESTIYA VUZOV SSSR, seriya "Radioelektronika," vol 20, No. 5, 1977.

3. Shelukhin, O. I. IZVESTIYA VUZOV SSSR, Seriya "Radioelektronika," Vol 21, No. 5, 1978.

[217-9194]

9194
CSO: 1860

- END -